

Hydrodynamics of Shocked Interfaces

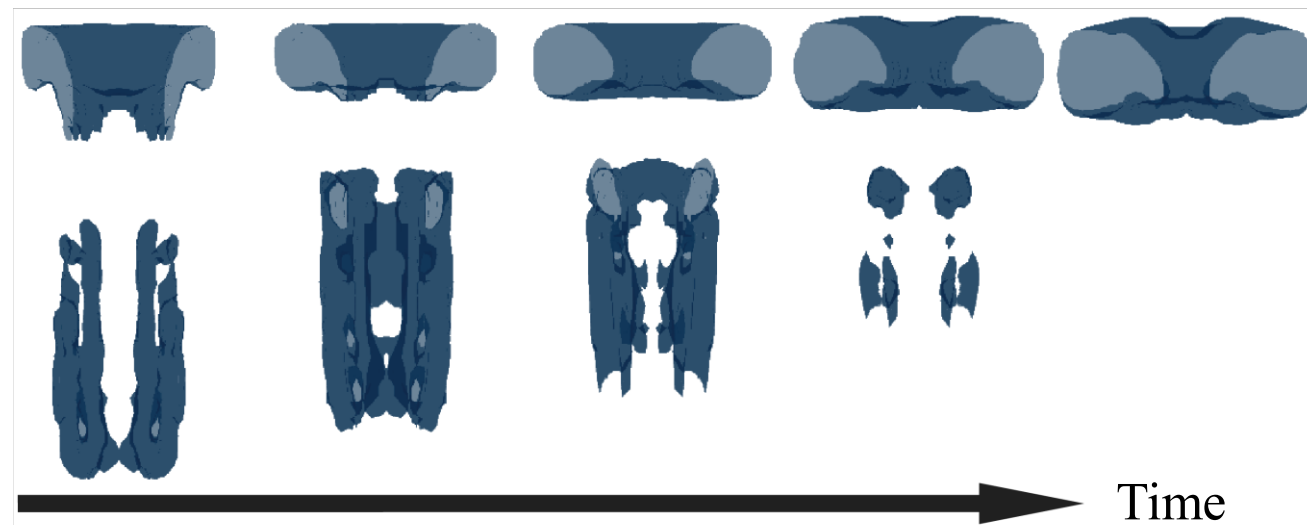


Michael Wadas
Department of Mechanical Engineering
University of Michigan, Ann Arbor



Summary

1. Shock waves occur in a wide range of engineering and scientific contexts including laser experiments, astrophysics, and inertial confinement fusion (ICF).
2. High-powered lasers can drive strong waves in materials, enabling their study in extreme pressure environments. We developed a method for further strengthening such shocks.
3. Shocked interfaces mix via the Richtmyer-Meshkov instability (RMI), possibly leading to the escape of high-vorticity ejecta with important implications for turbulent transitions.

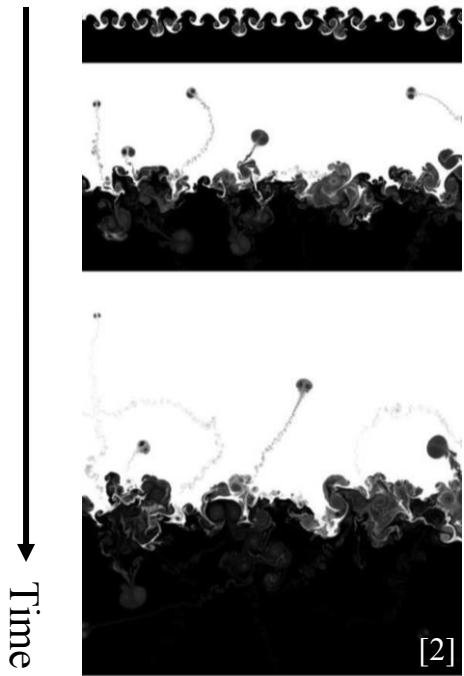
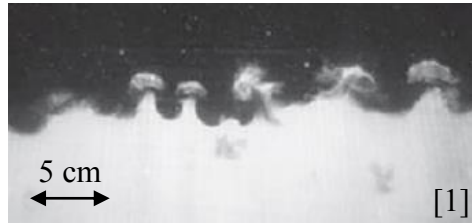


Shock waves occur in a variety of engineering and natural contexts where they interact with fluid interfaces.

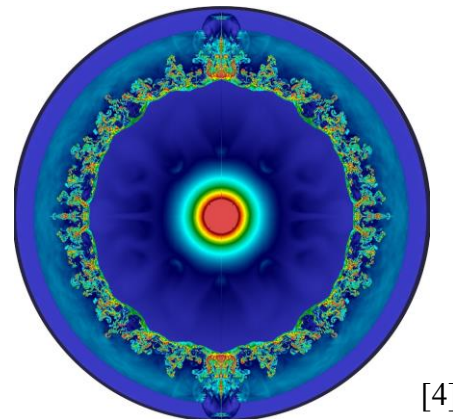
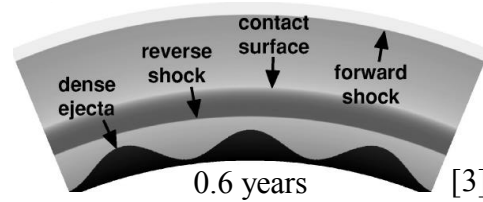
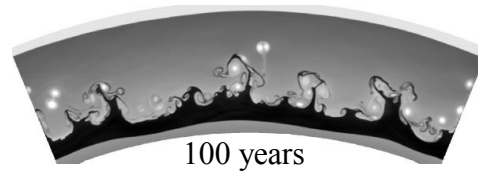
Compression Experiments



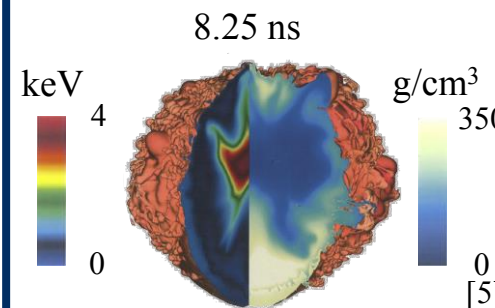
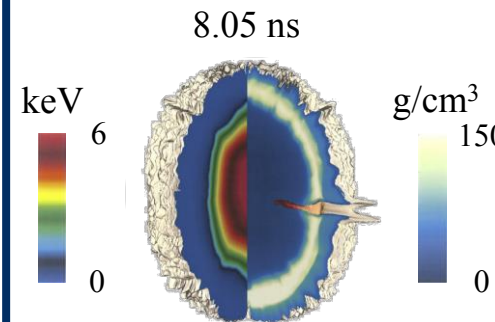
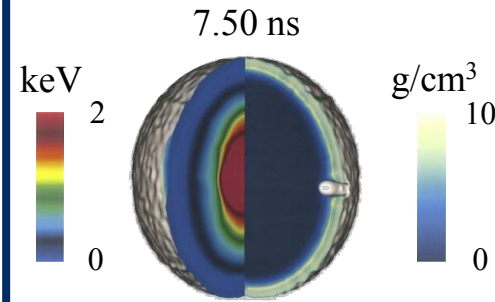
Richtmyer-Meshkov Instability (RMI)



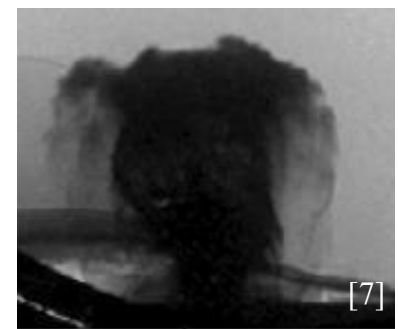
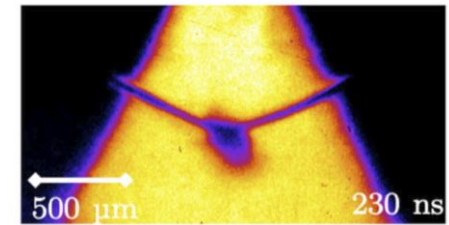
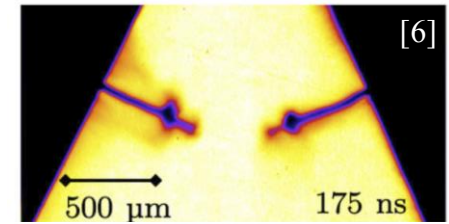
Supernovae



Inertial Confinement Fusion (ICF)



Ejecta/Jet Physics

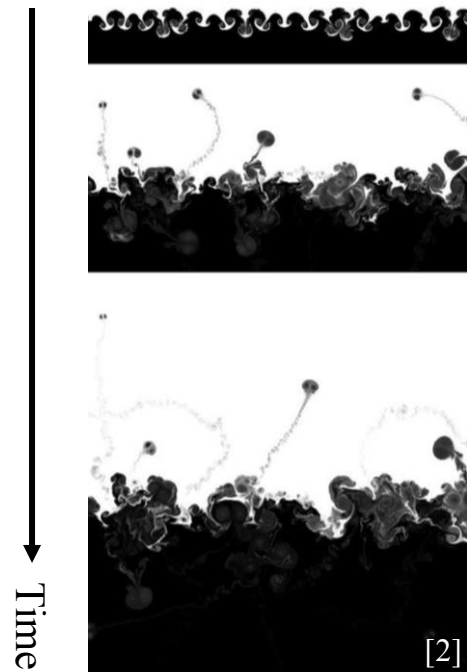
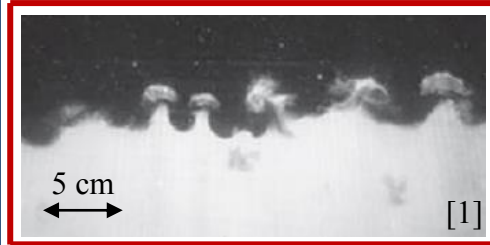


Shock waves occur in a variety of engineering and natural contexts where they interact with fluid interfaces.

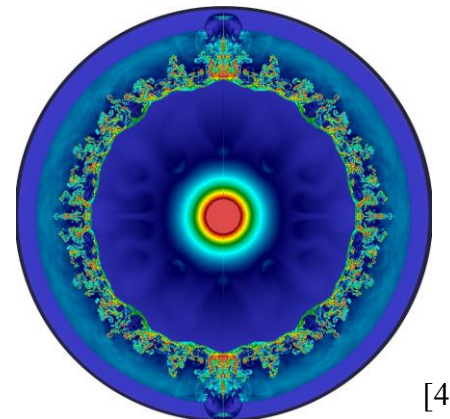
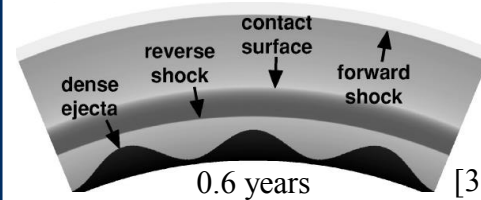
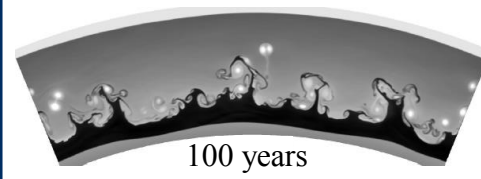
Compression Experiments



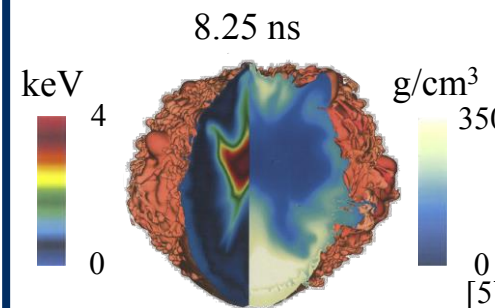
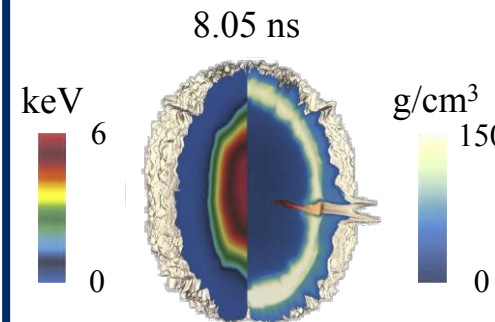
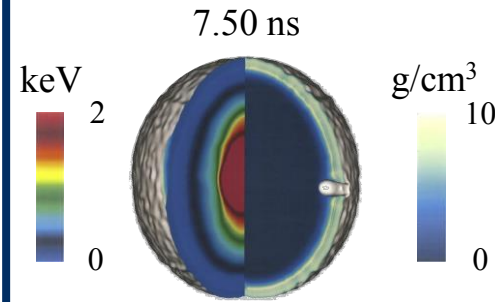
Richtmyer-Meshkov Instability (RMI)



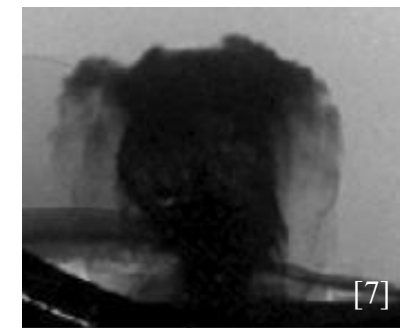
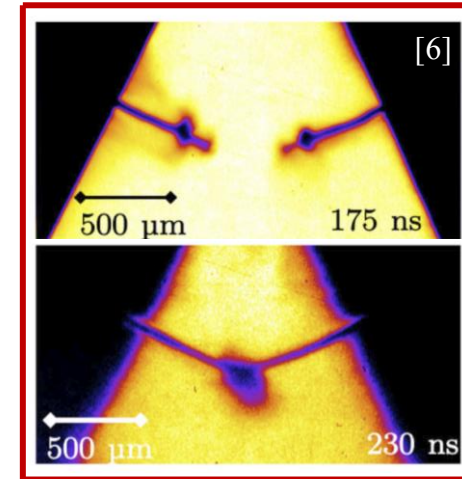
Supernovae



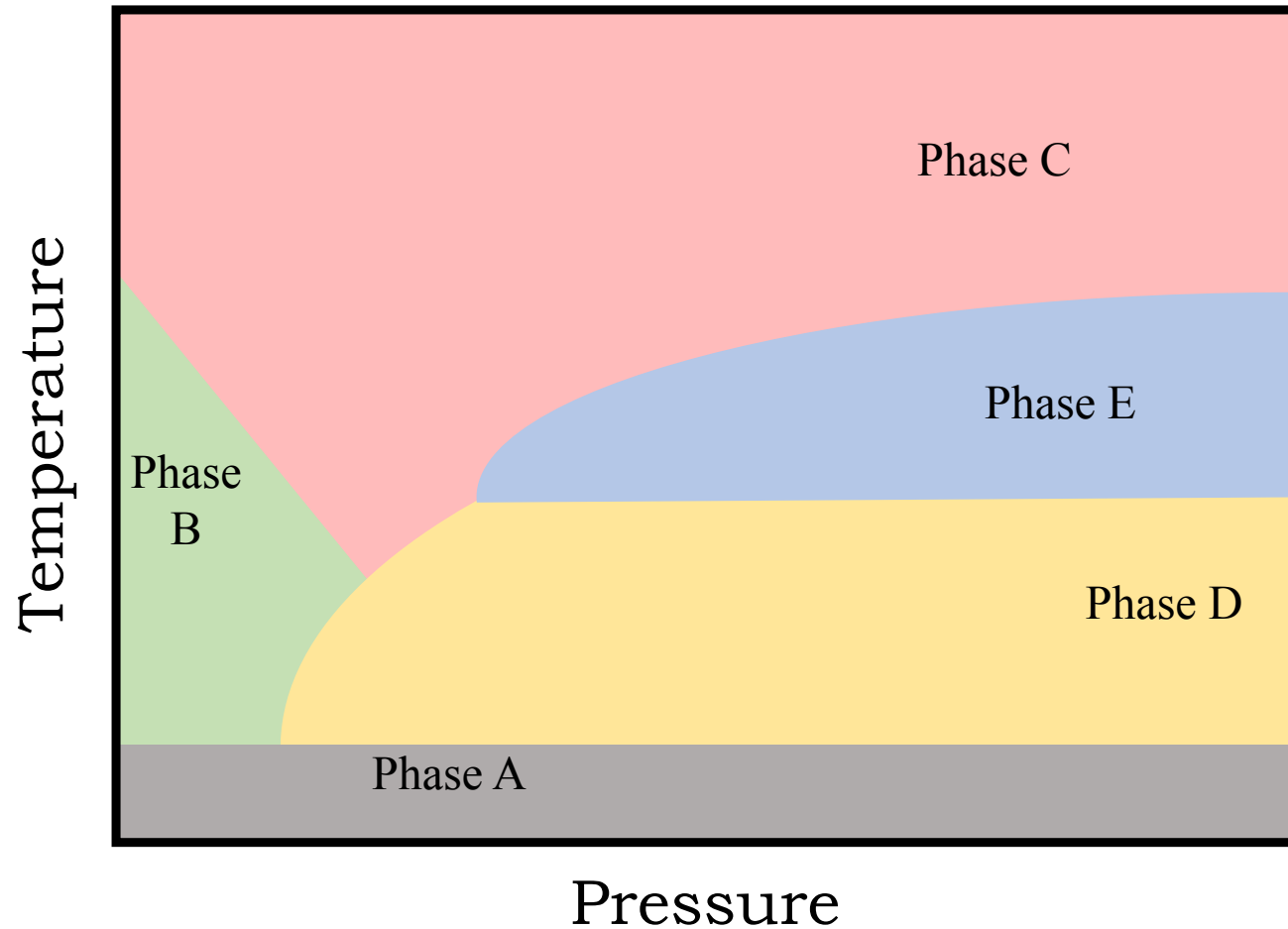
Inertial Confinement Fusion (ICF)



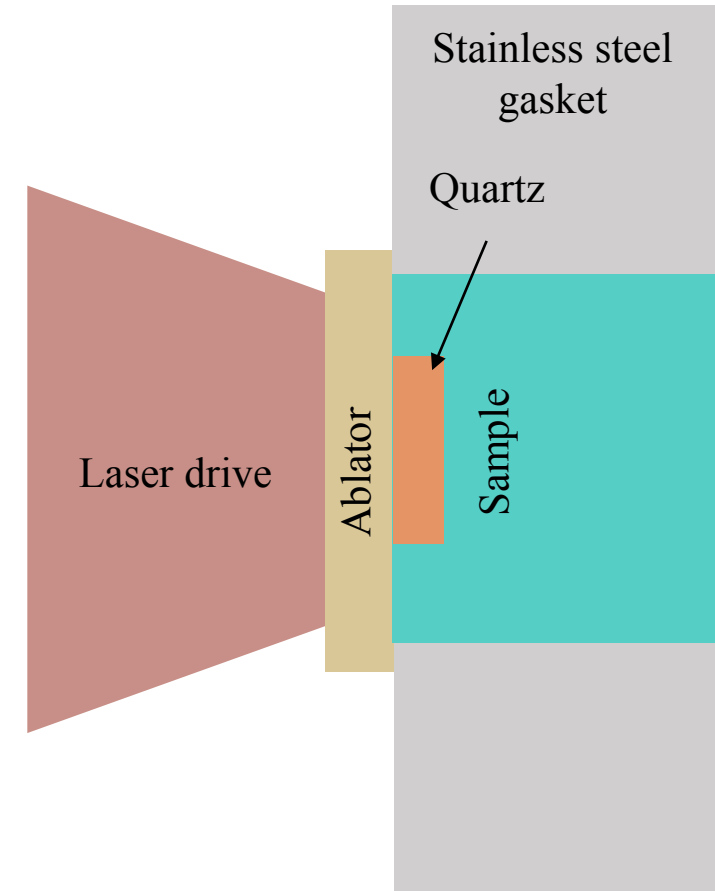
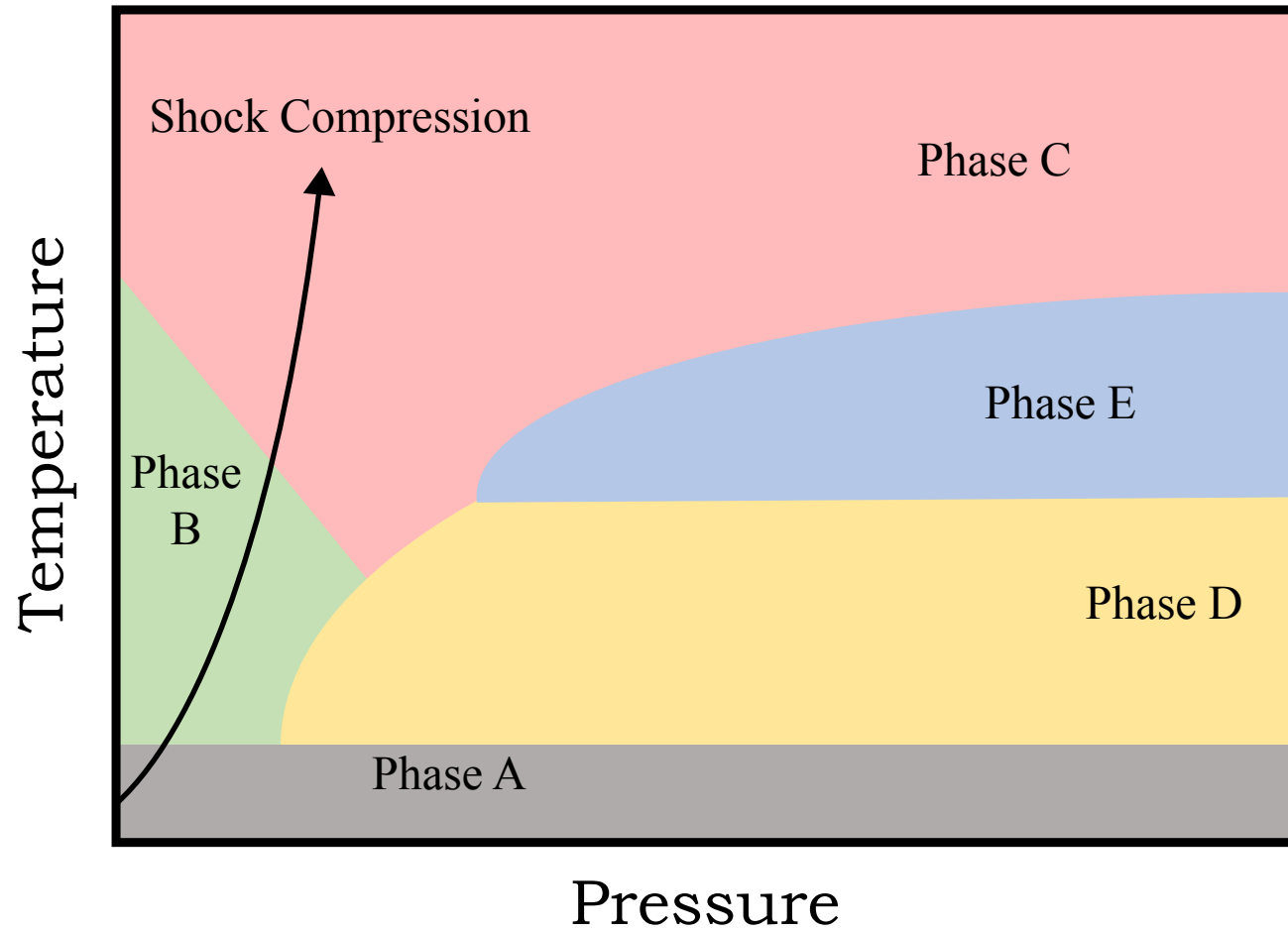
Ejecta/Jet Physics



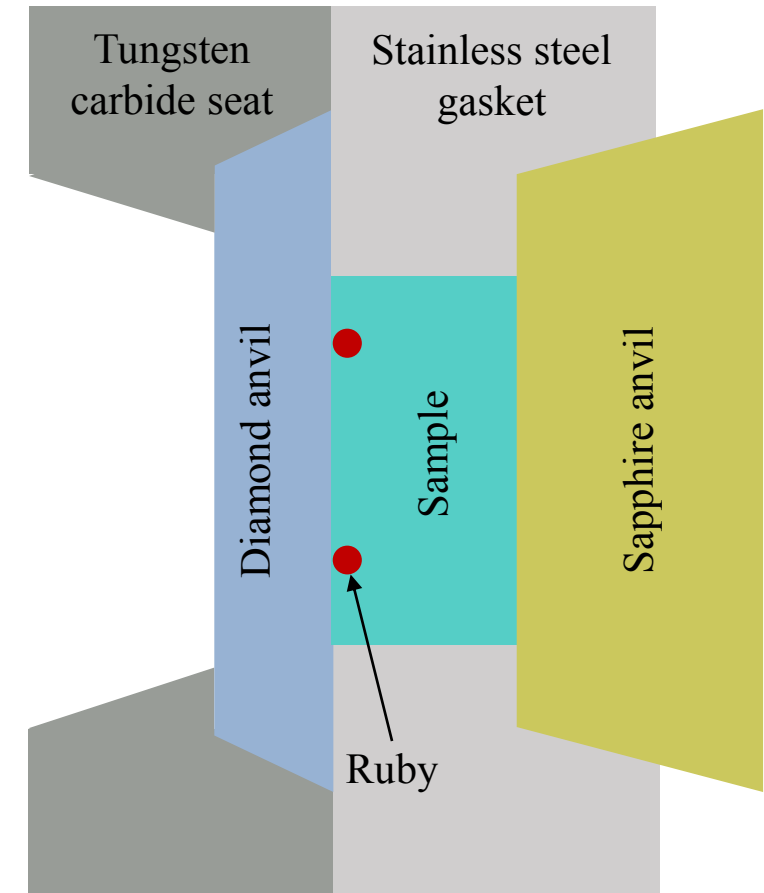
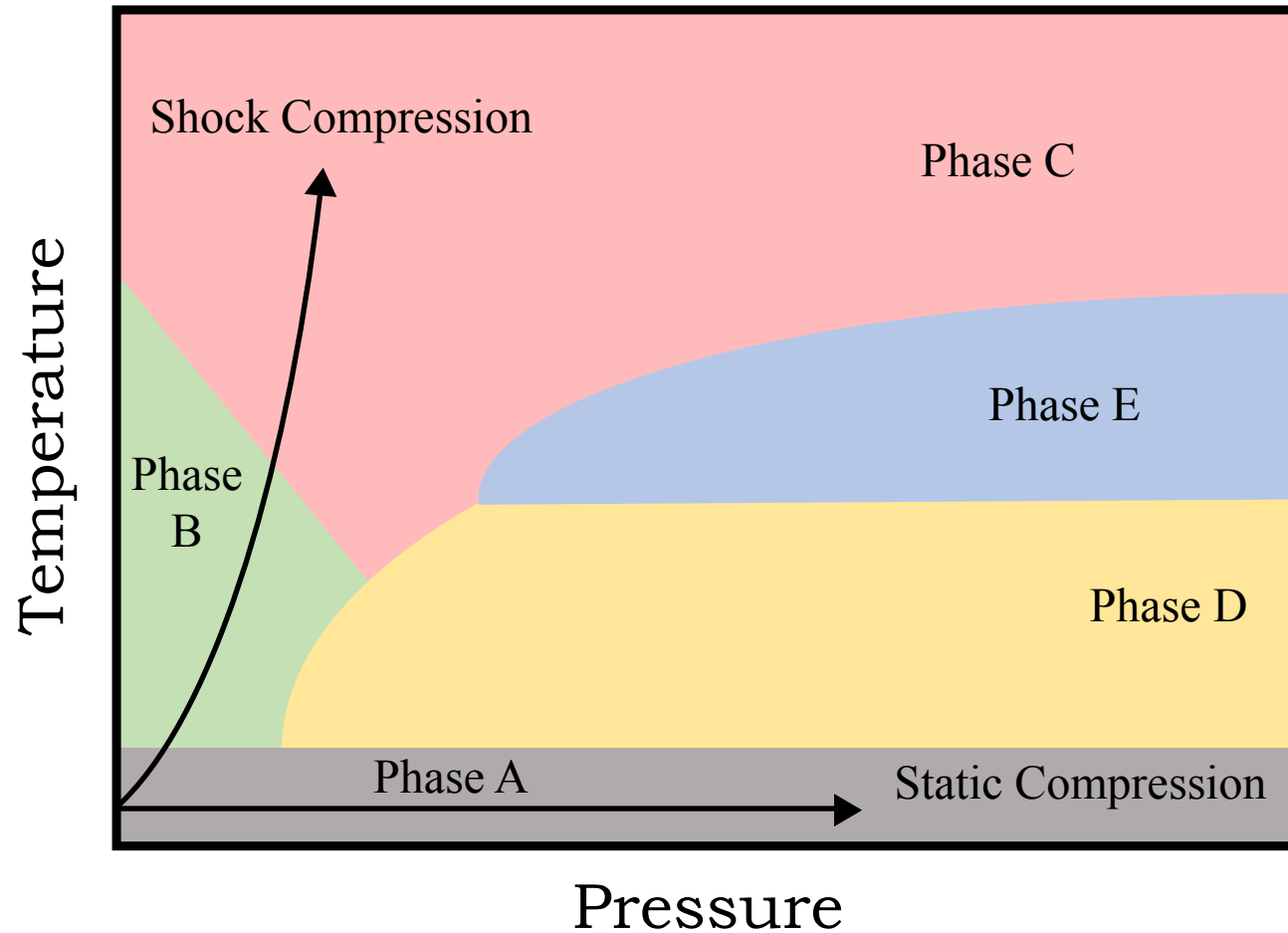
Dynamic compression experiments utilize lasers to generate shocks that compress materials to extreme pressures in a nominally 1D system.



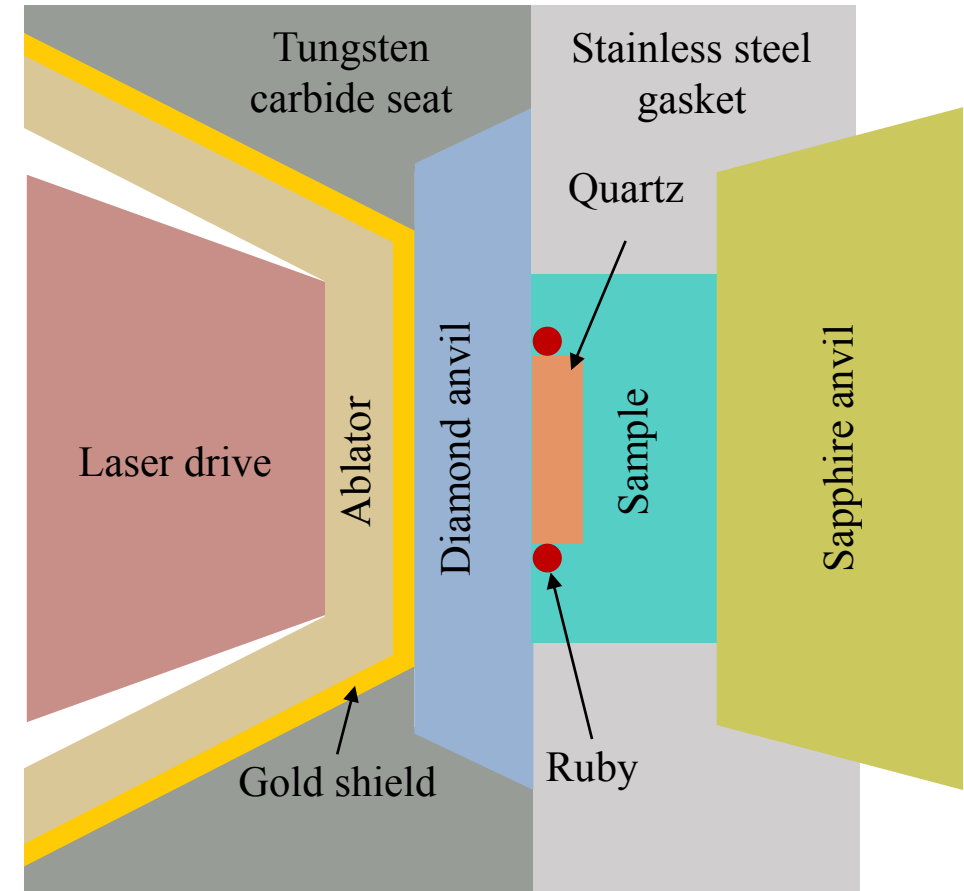
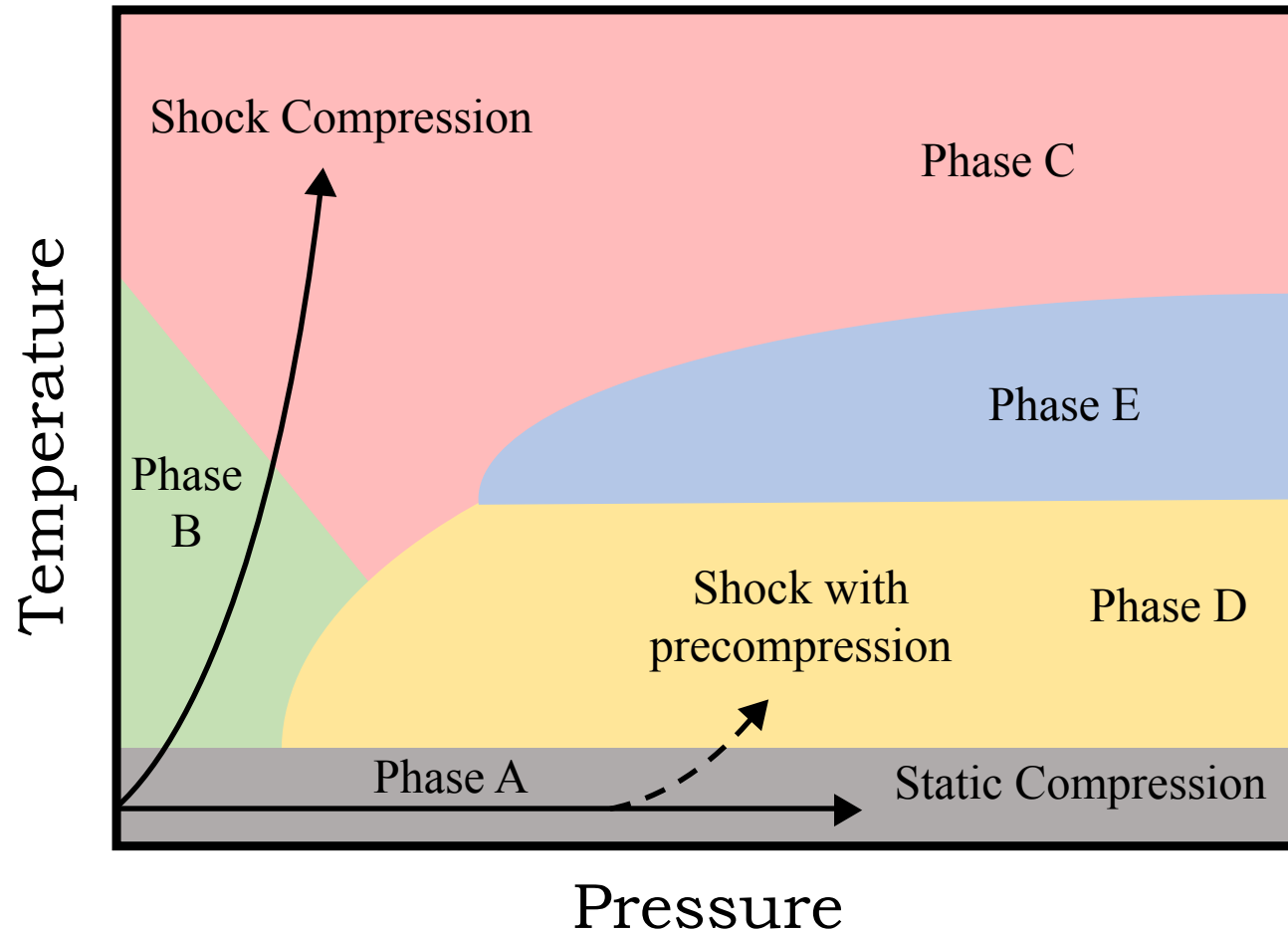
Dynamic compression experiments utilize lasers to generate shocks that compress materials to extreme pressures in a nominally 1D system.



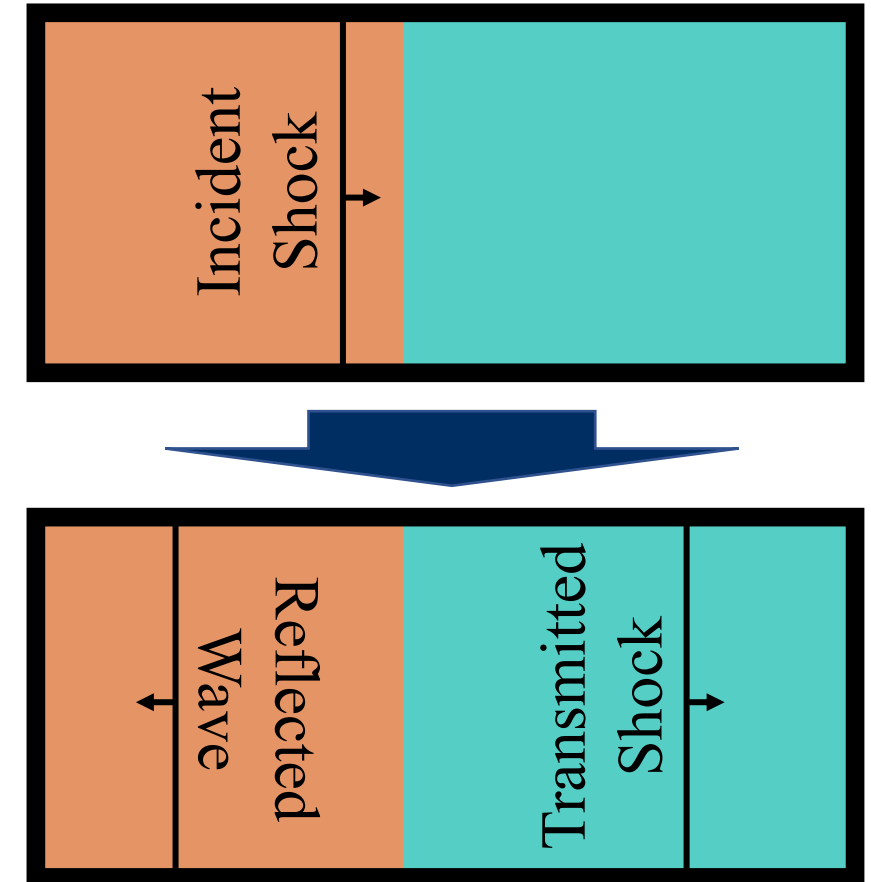
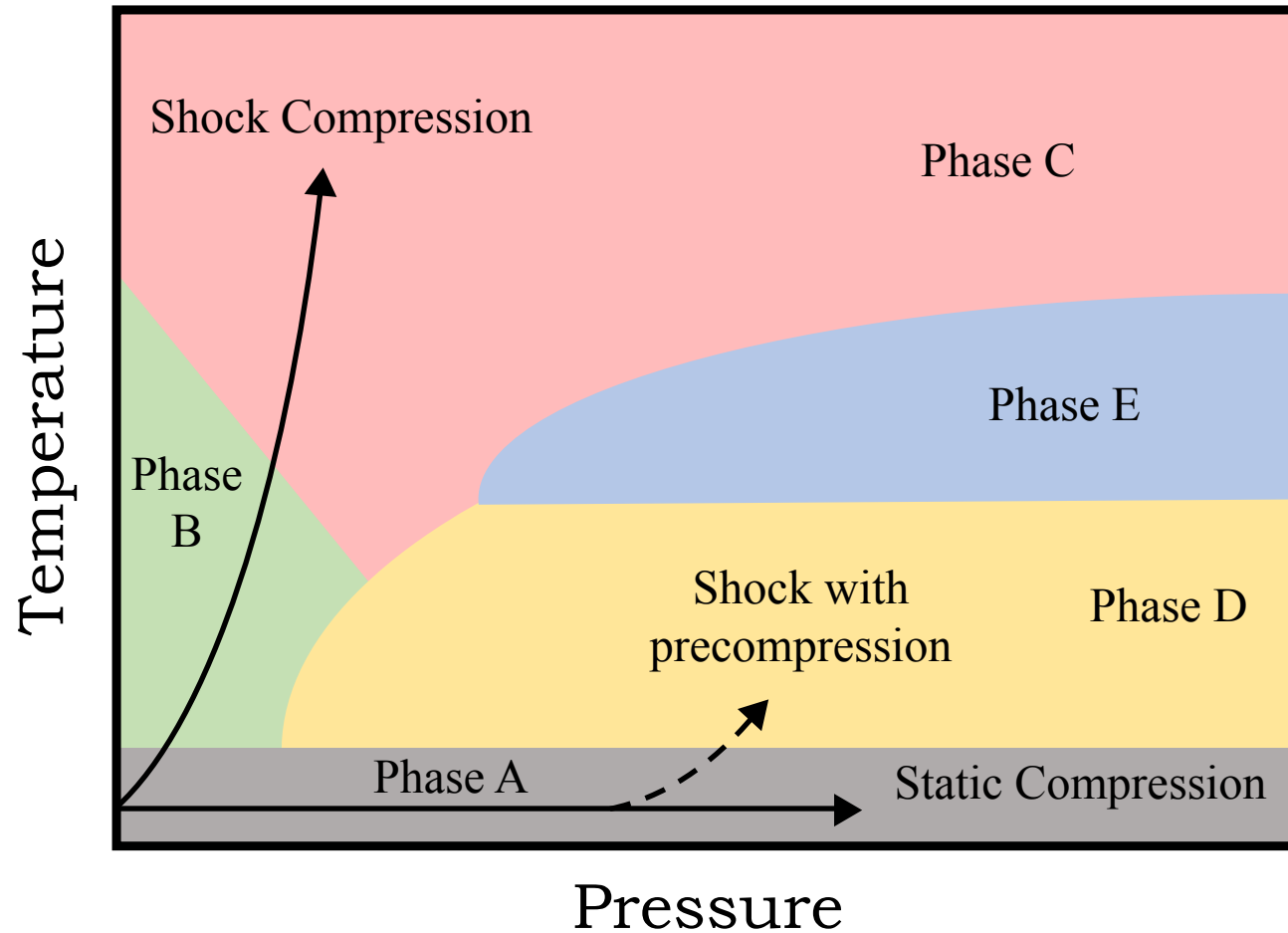
Dynamic compression experiments utilize lasers to generate shocks that compress materials to extreme pressures in a nominally 1D system.



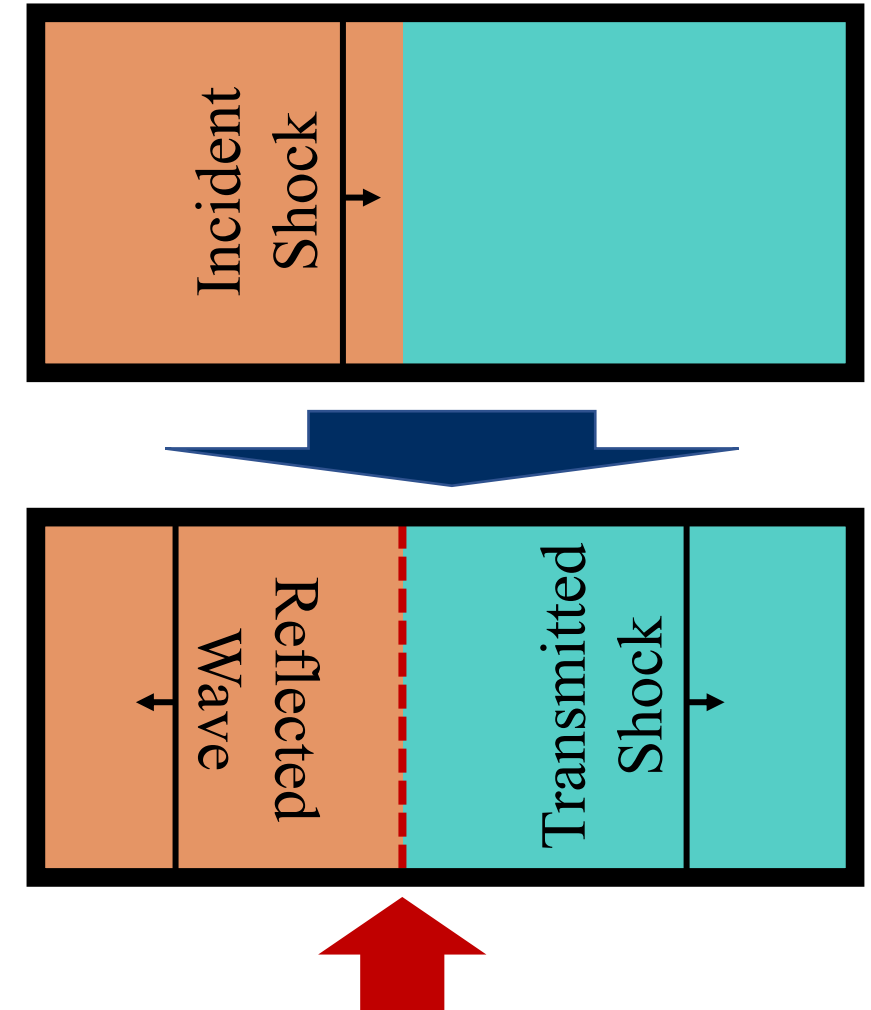
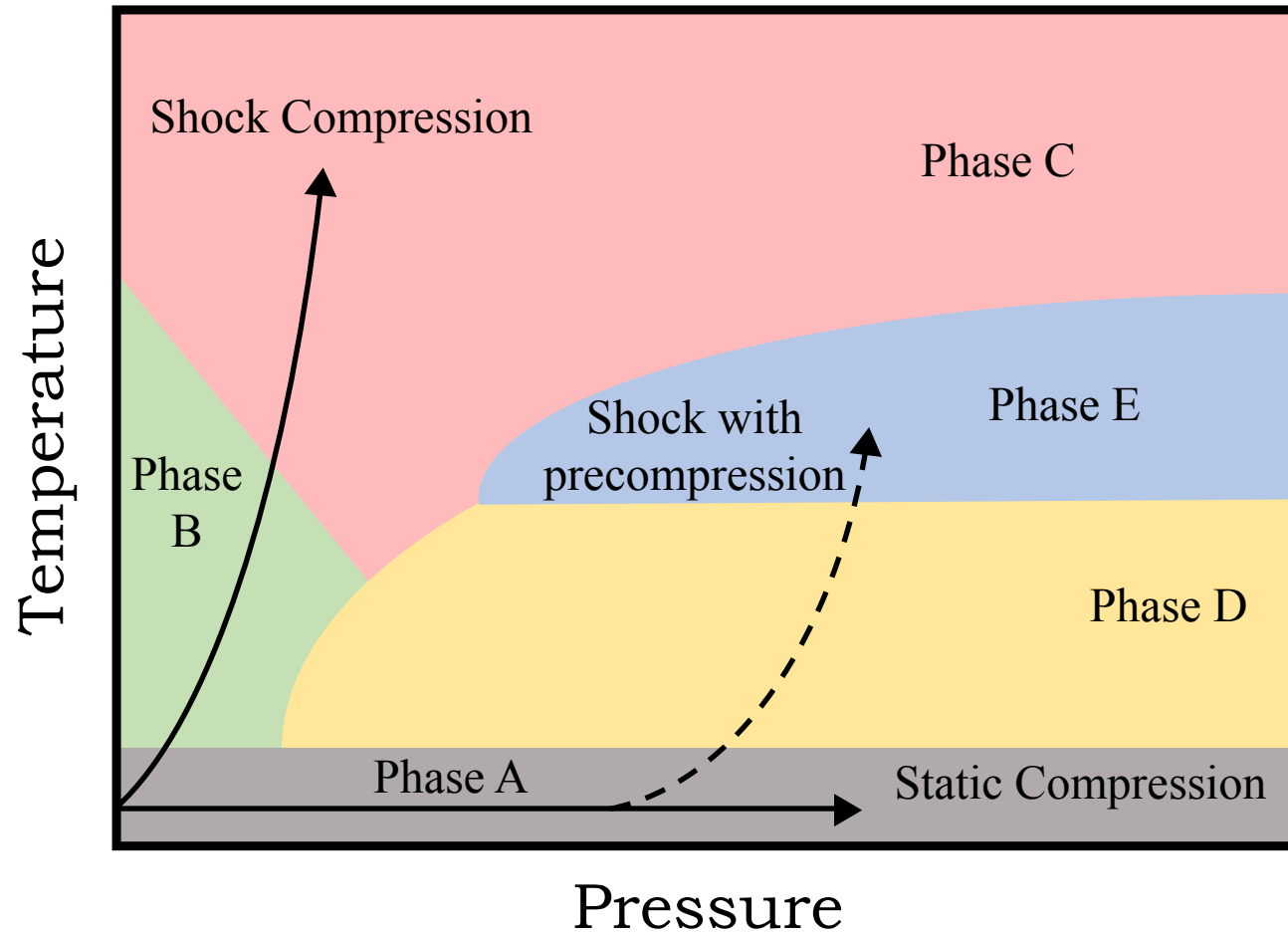
Dynamic compression experiments utilize lasers to generate shocks that compress materials to extreme pressures in a nominally 1D system.



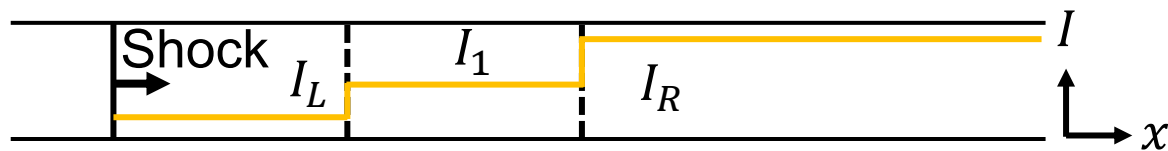
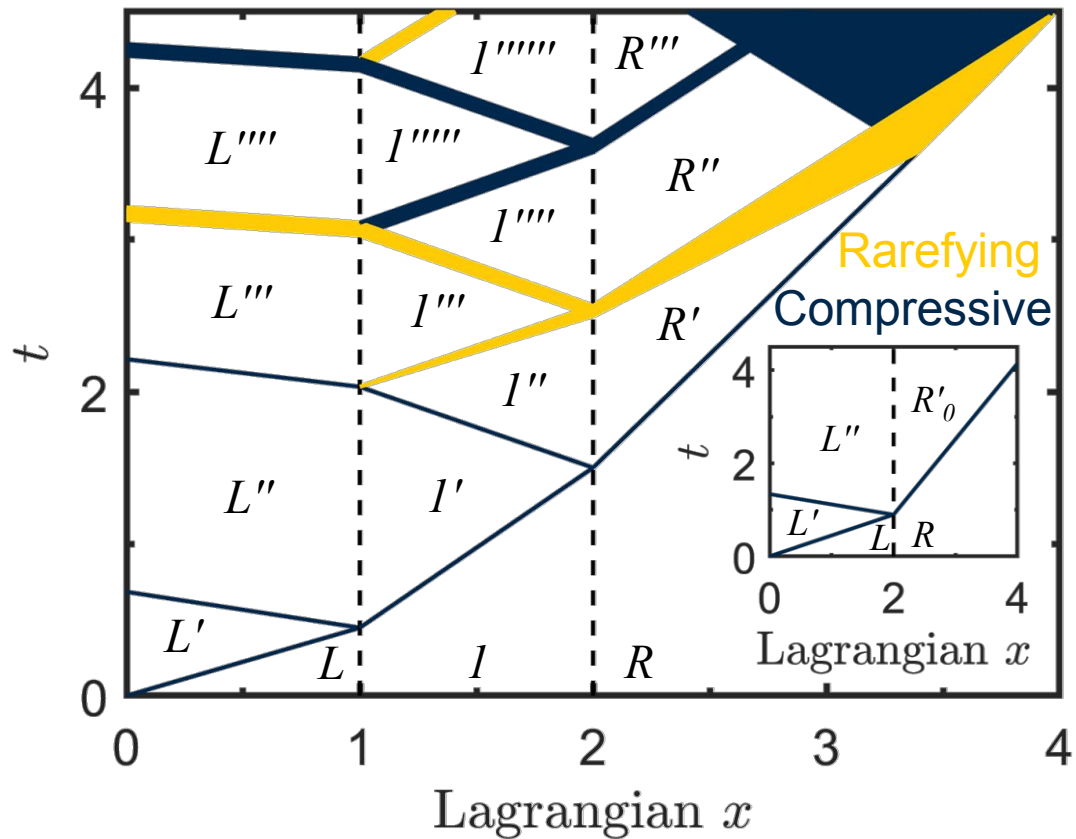
Dynamic compression experiments utilize lasers to generate shocks that compress materials to extreme pressures in a nominally 1D system.



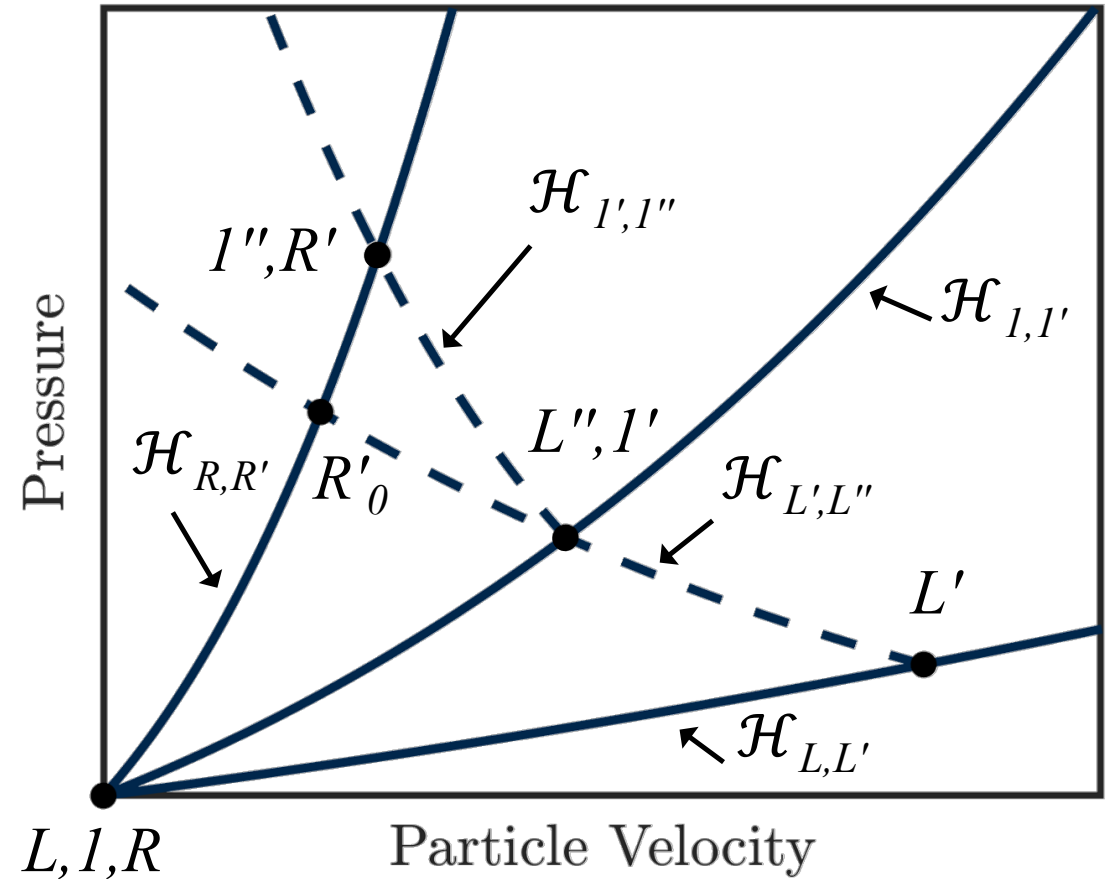
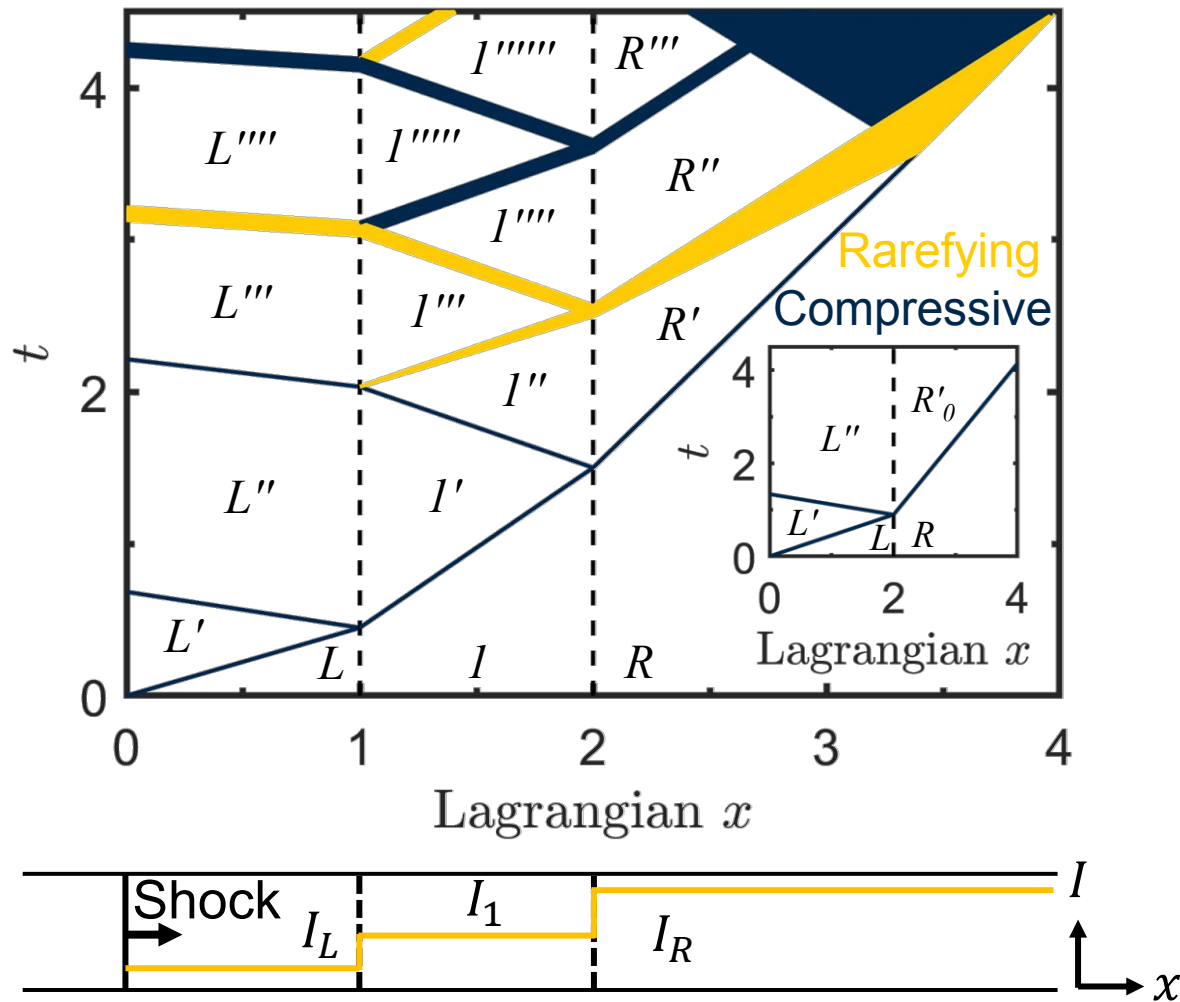
Dynamic compression experiments utilize lasers to generate shocks that compress materials to extreme pressures in a nominally 1D system.



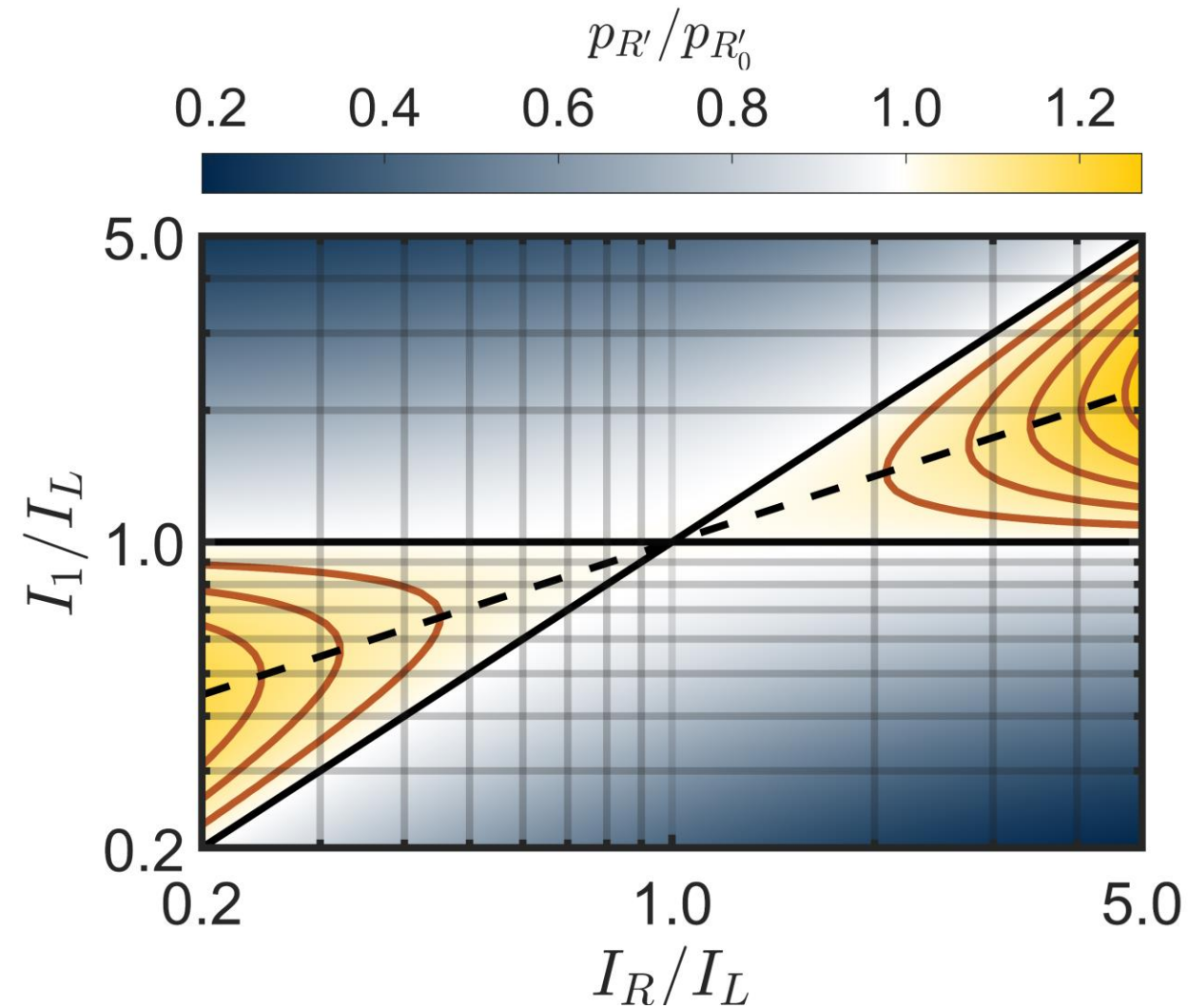
An intermediate material bridging an impedance discontinuity can transiently strengthen a shock wave in a material of interest.



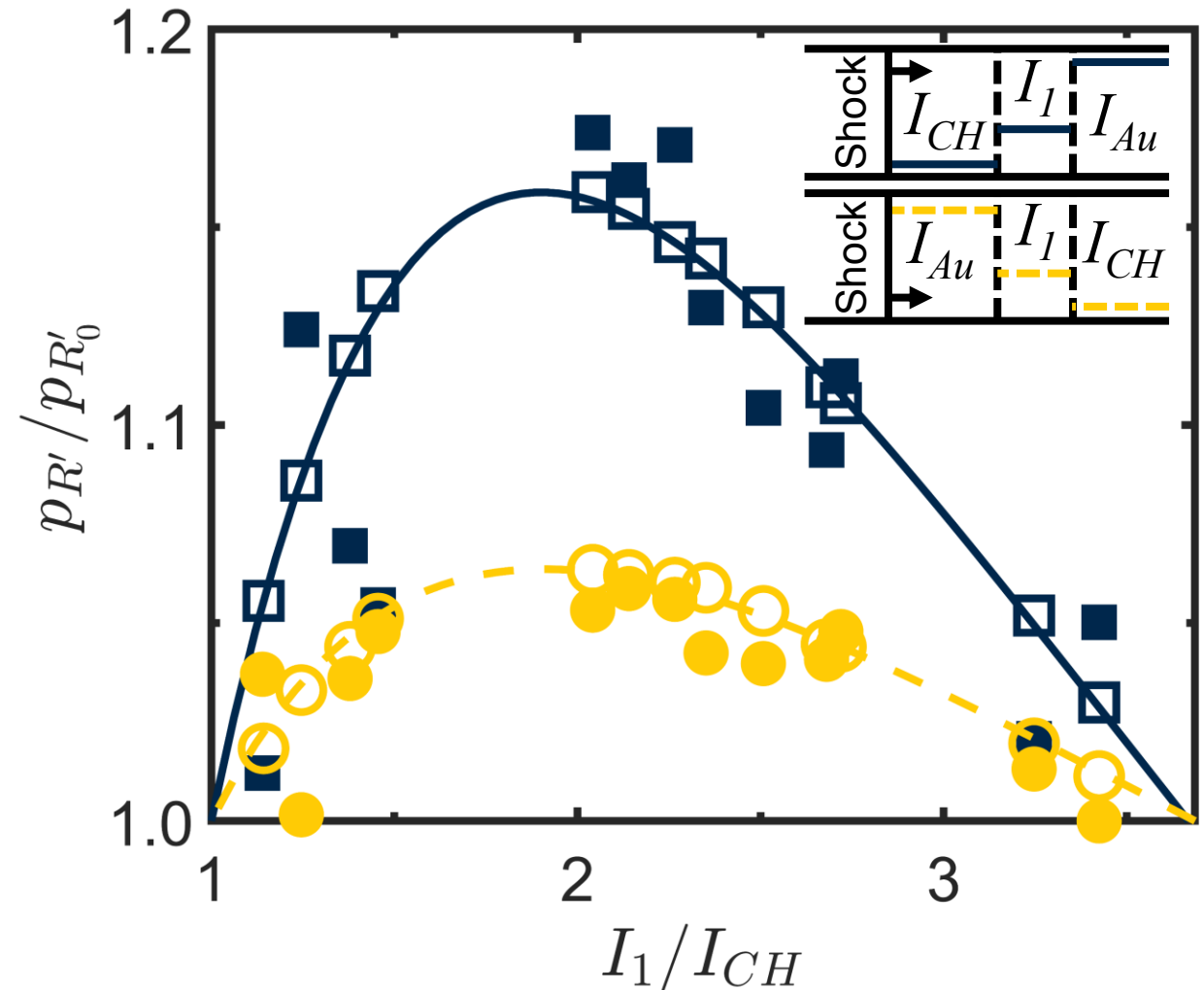
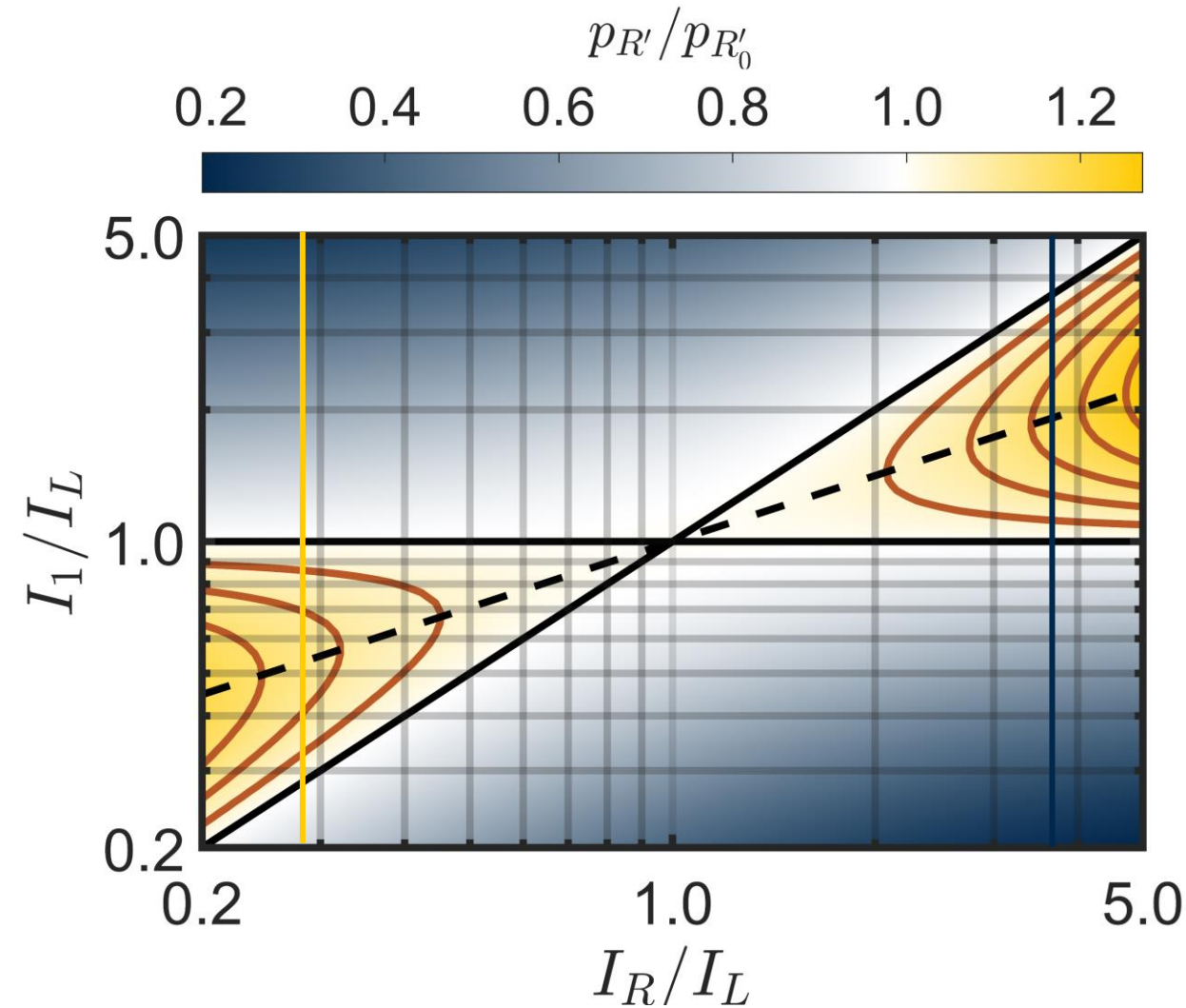
An intermediate material bridging an impedance discontinuity can transiently strengthen a shock wave in a material of interest.



A single intermediate material can increase pressures by up to 16%, as verified by HYADES simulations utilizing tabular equations of state.

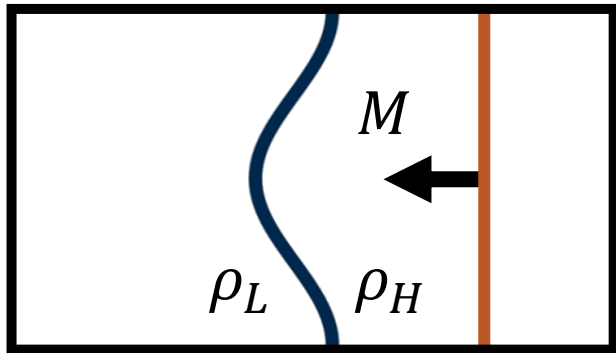


A single intermediate material can increase pressures by up to 16%, as verified by HYADES simulations utilizing tabular equations of state.

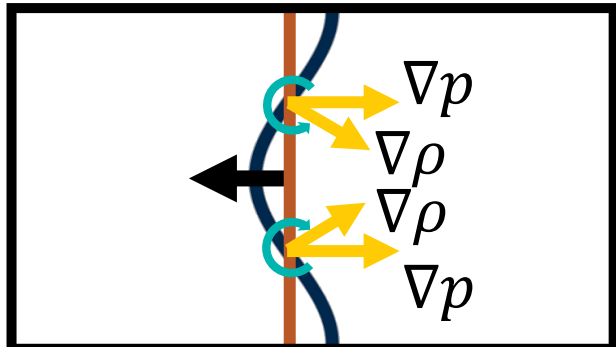


[8]

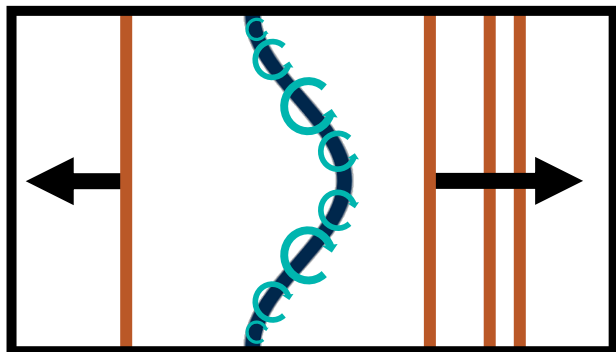
Energy and circulation deposited when a shock wave passes through a perturbed interface leads to significant interfacial mixing.



Shock impinges on heavy-to-light interface

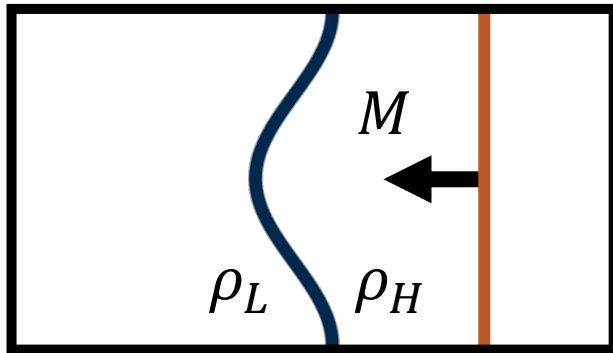


Shock deposits baroclinic vorticity

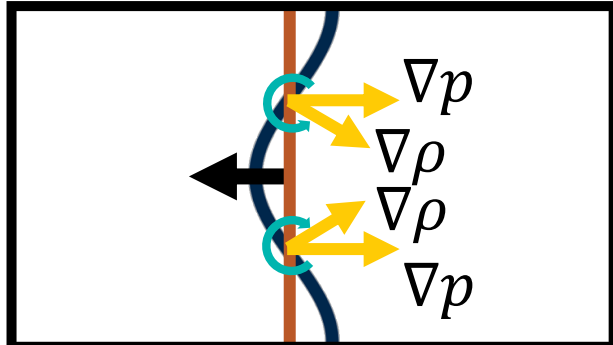
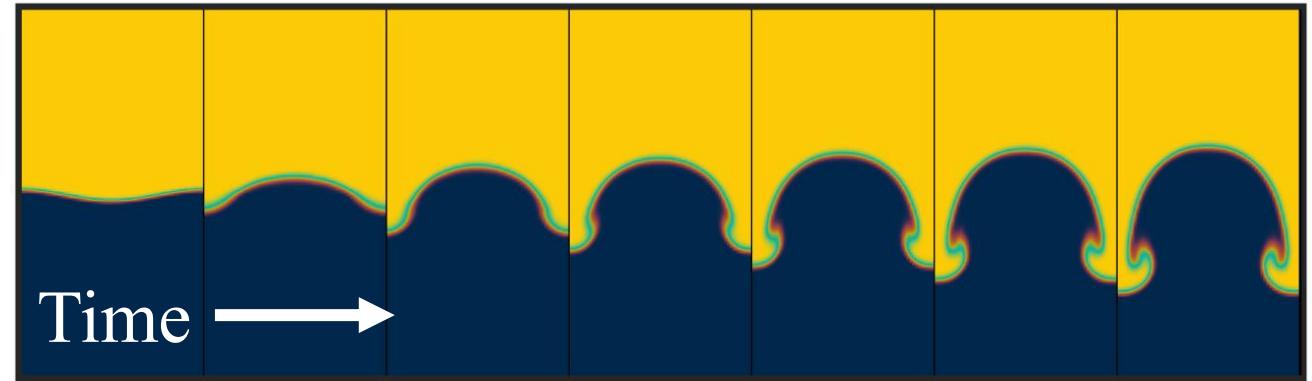


Rarefaction reflects and interface evolves

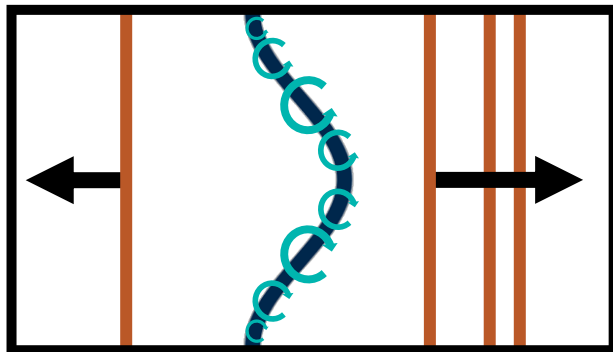
Energy and circulation deposited when a shock wave passes through a perturbed interface leads to significant interfacial mixing.



Shock impinges on heavy-to-light interface



Shock deposits baroclinic vorticity

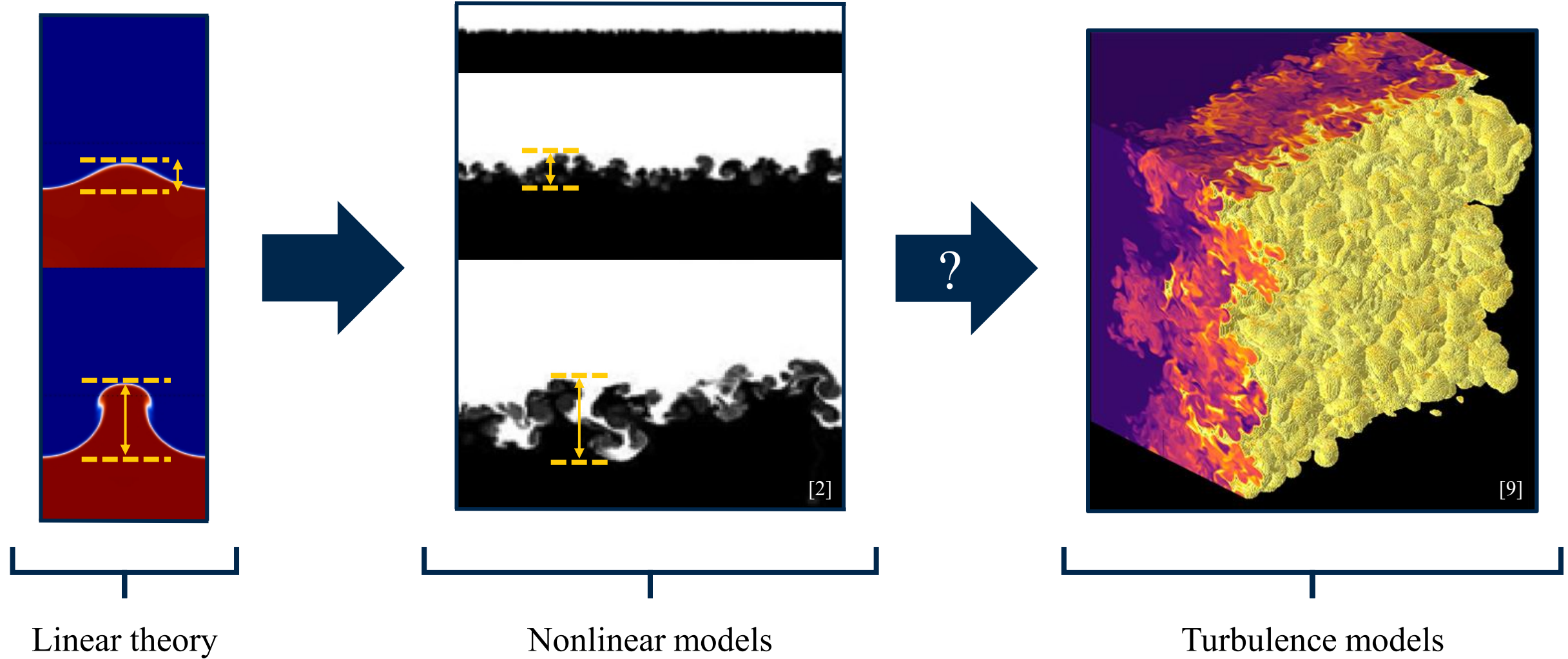


Rarefaction reflects and interface evolves

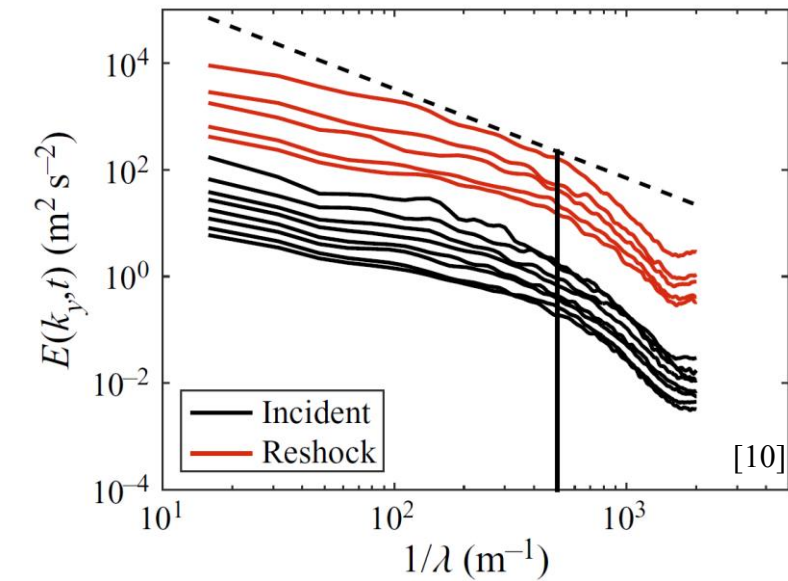
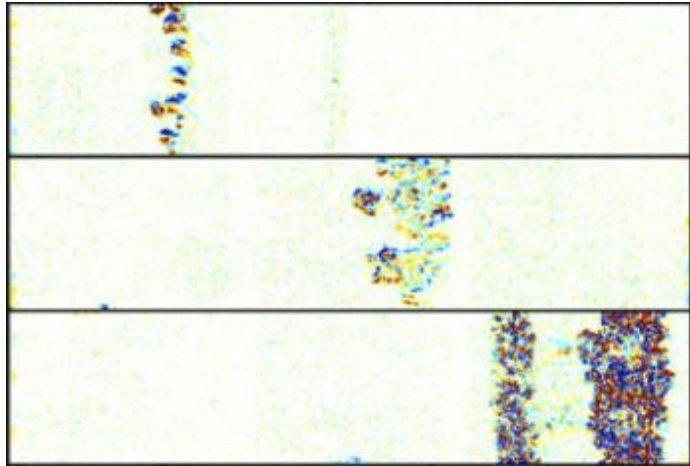


[1]

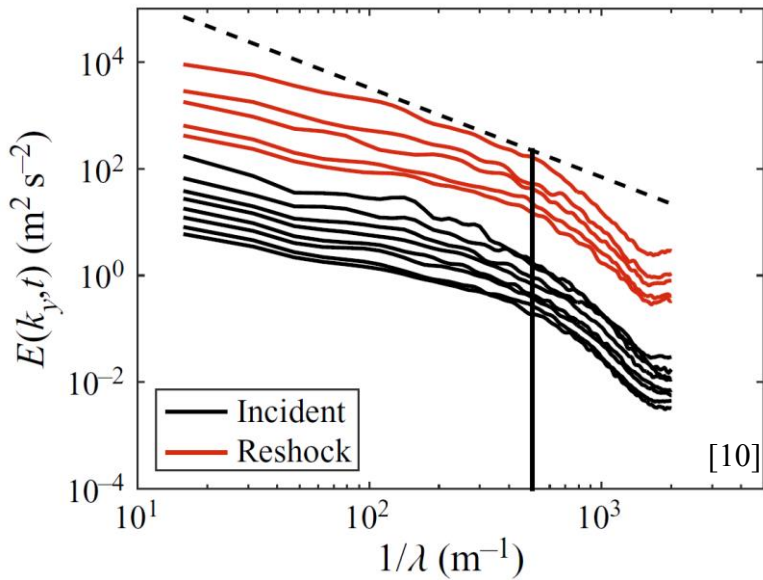
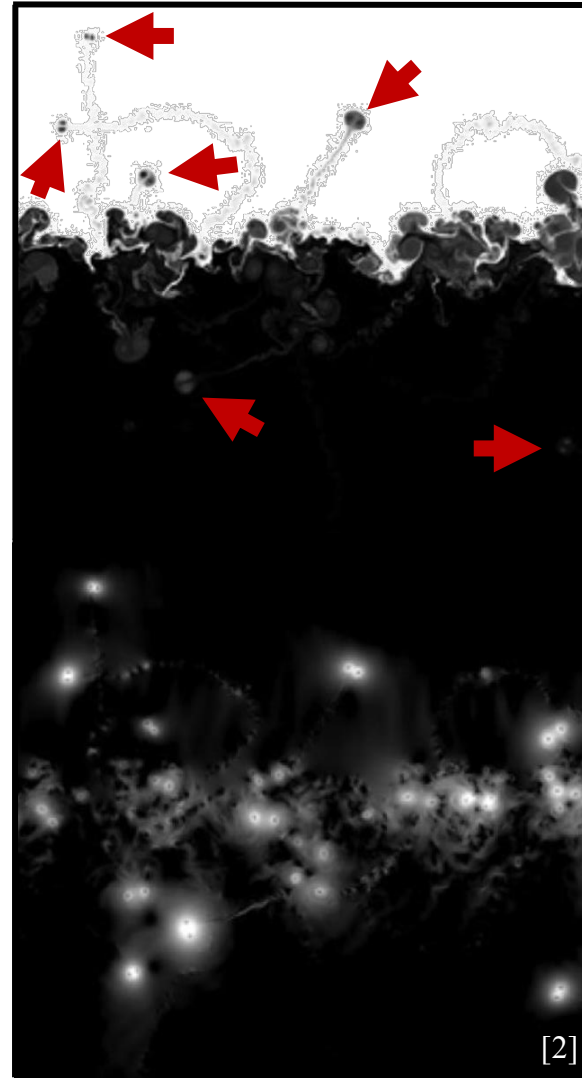
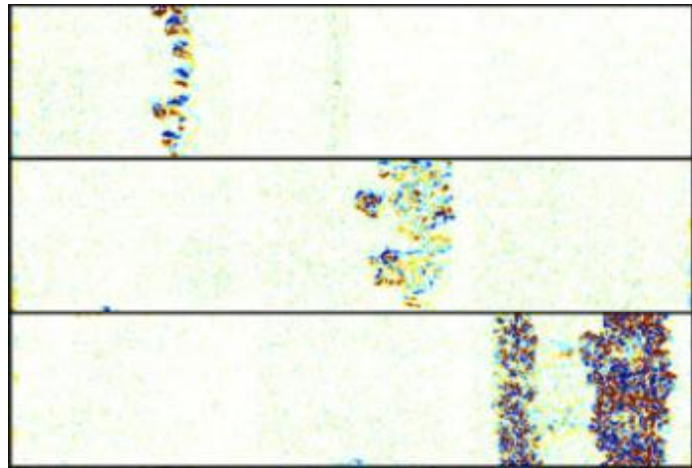
Linear theory and nonlinear models predict the width of the mixing layer for multimode interfaces, with an eventual handoff to turbulence models.



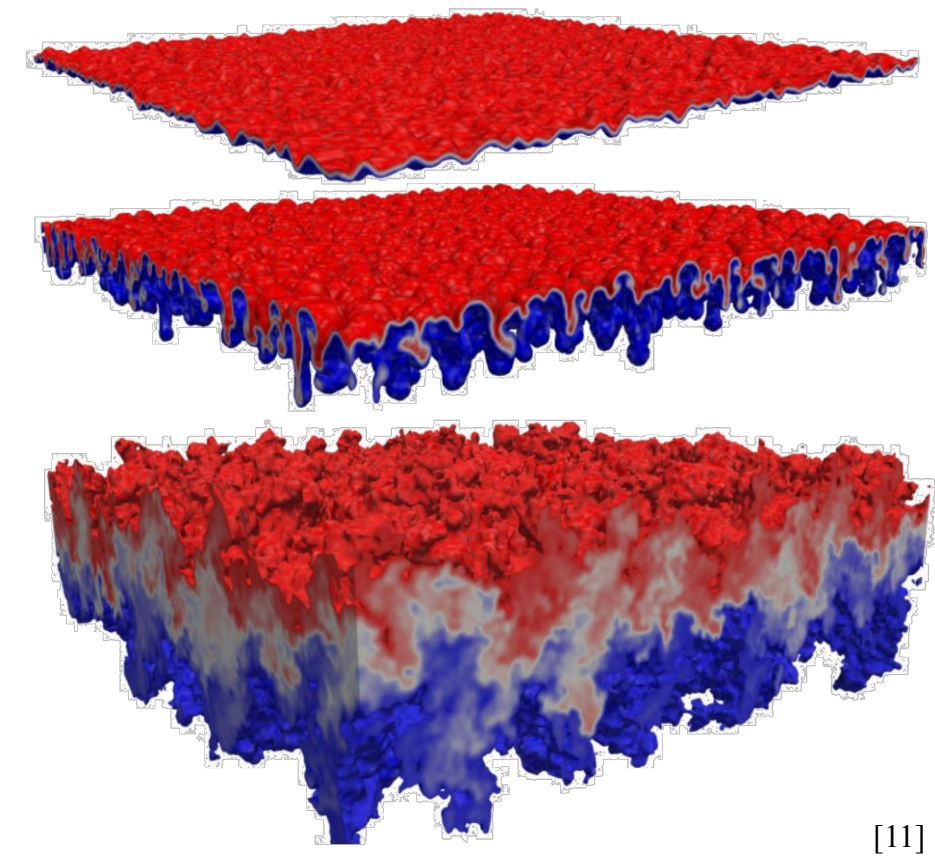
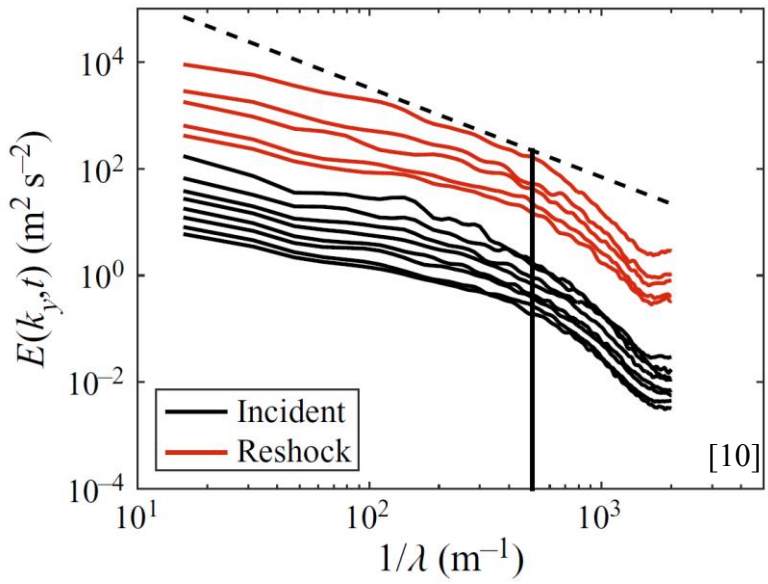
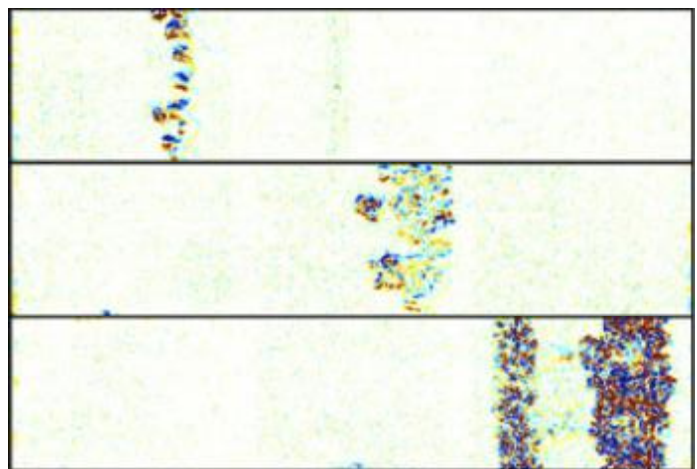
The transition to turbulence of the RMI is not well understood and involves several complicating transport mechanisms.



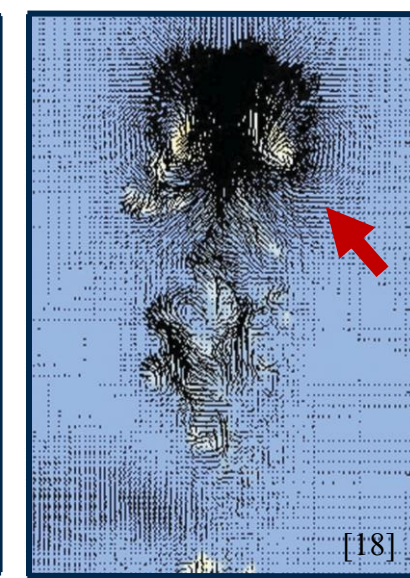
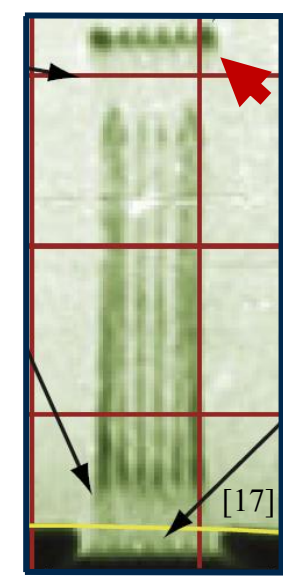
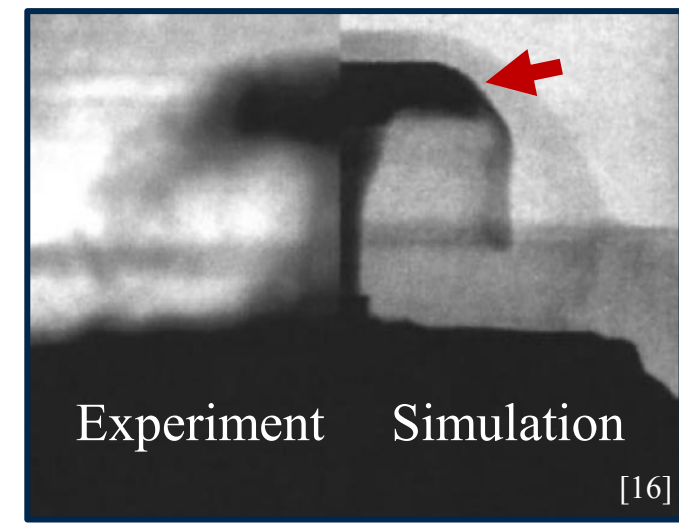
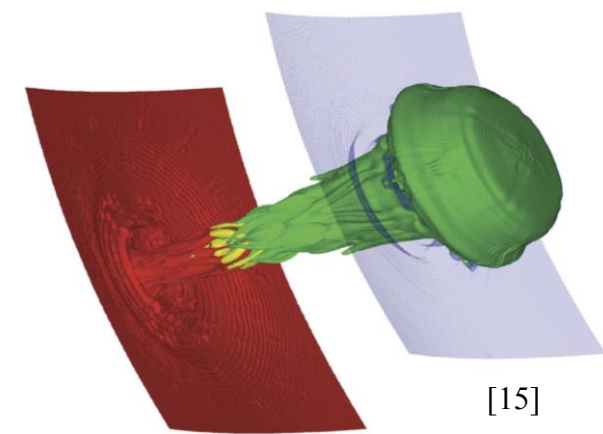
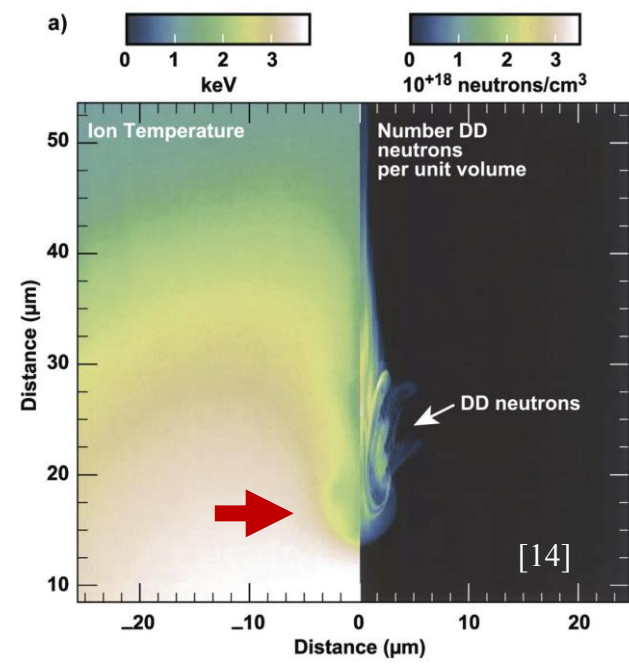
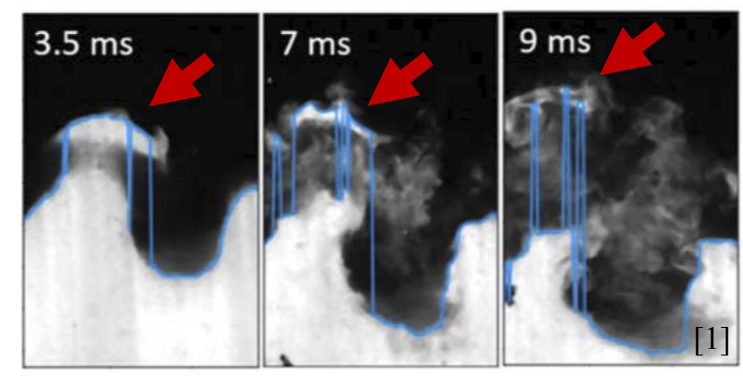
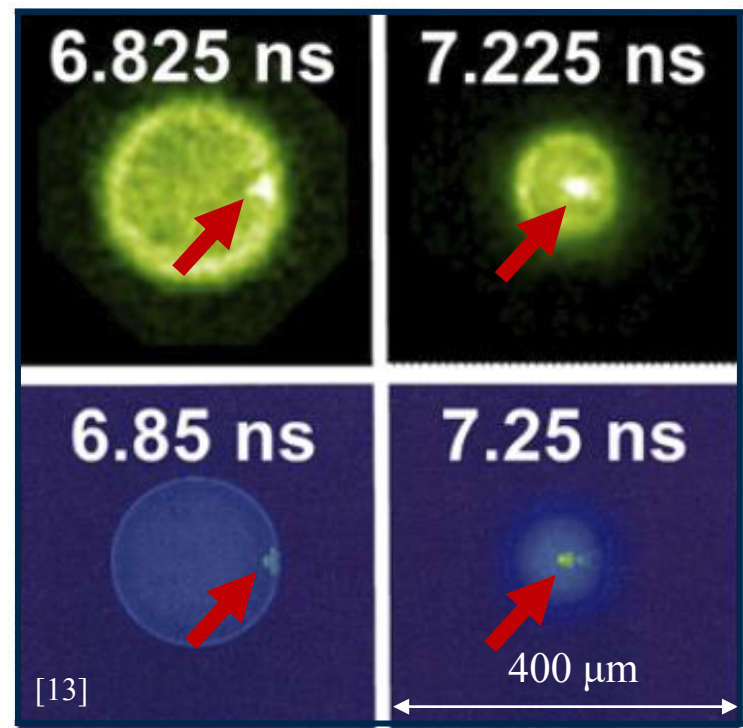
The transition to turbulence of the RMI is not well understood and involves several complicating transport mechanisms.



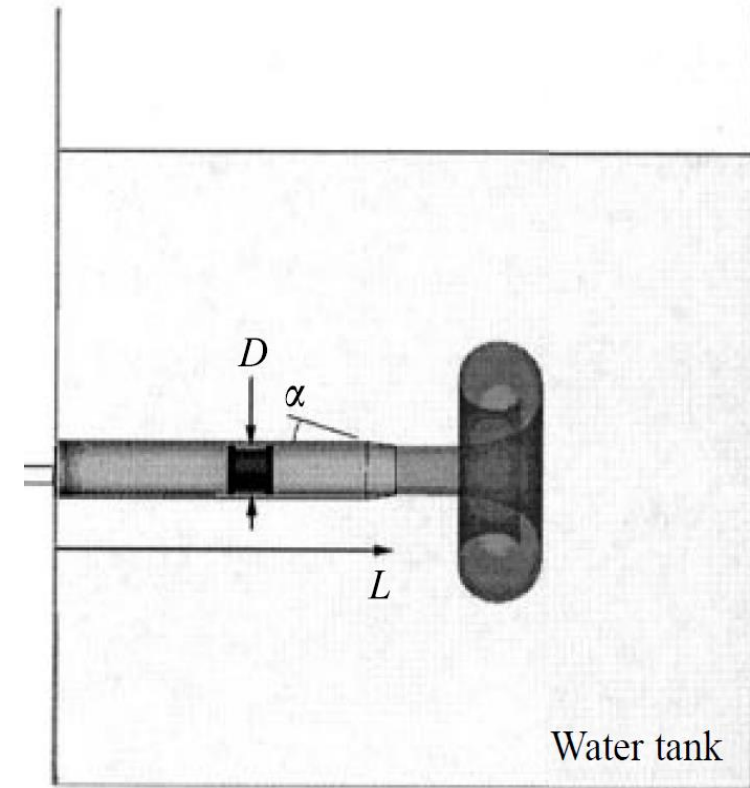
The transition to turbulence of the RMI is not well understood and involves several complicating transport mechanisms.



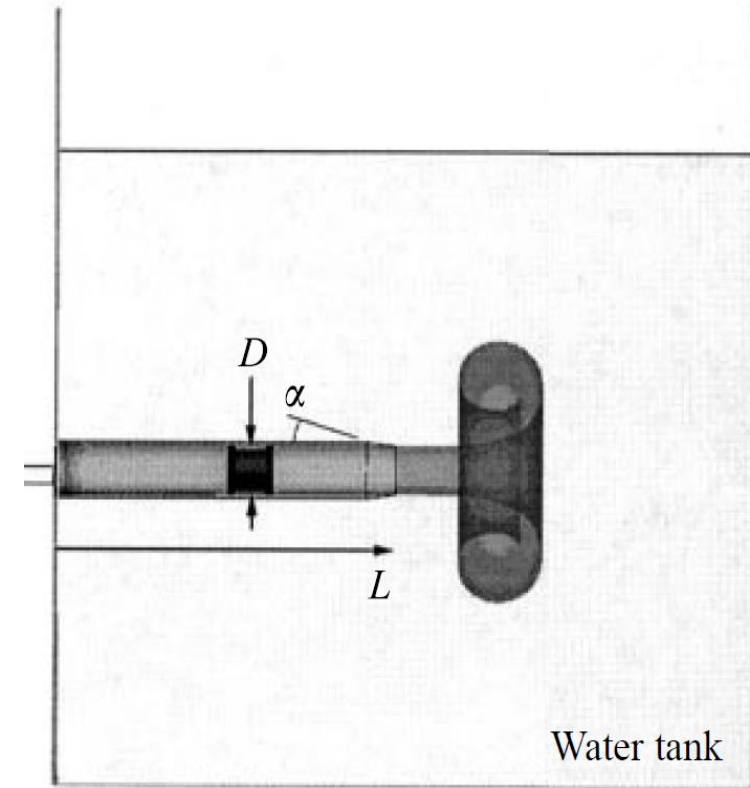
In addition to the RMI, shocked interfaces can generate jet/ejecta flows with important applications in ICF, ejecta physics, and astrophysical jets.



Classical studies focus on vortex rings generated in a piston-cylinder apparatus and have uncovered key insights into their scaling behavior.



Classical studies focus on vortex rings generated in a piston-cylinder apparatus and have uncovered key insights into their scaling behavior.



$L/D = 2.0$



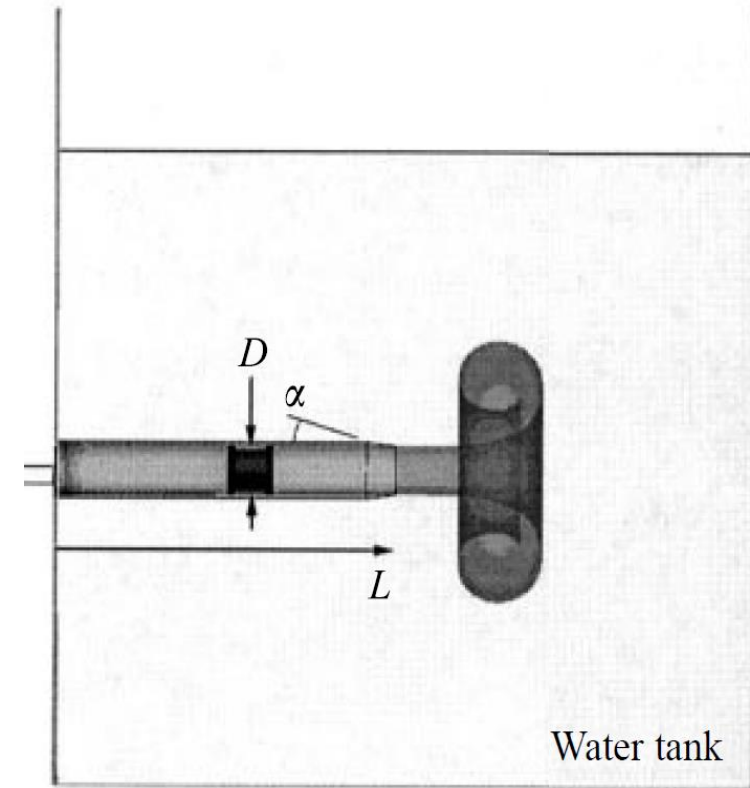
$L/D = 3.8$



$L/D = 14.5$



Classical studies focus on vortex rings generated in a piston-cylinder apparatus and have uncovered key insights into their scaling behavior.



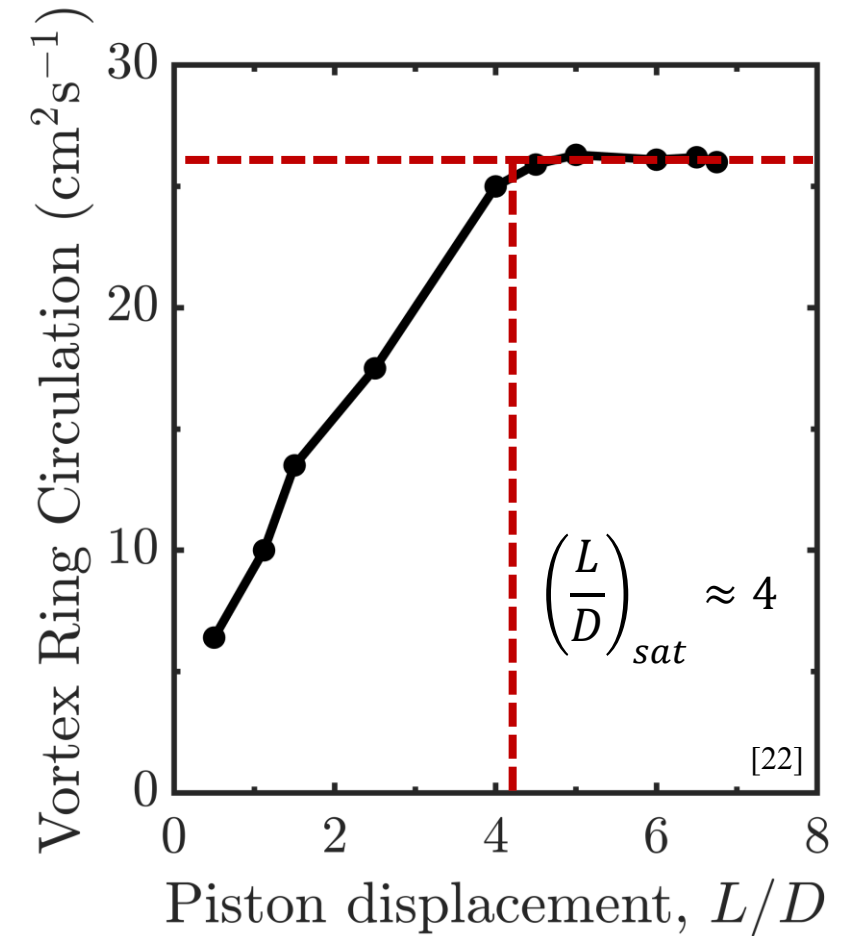
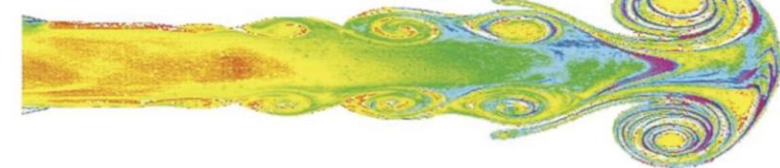
$L/D = 2.0$



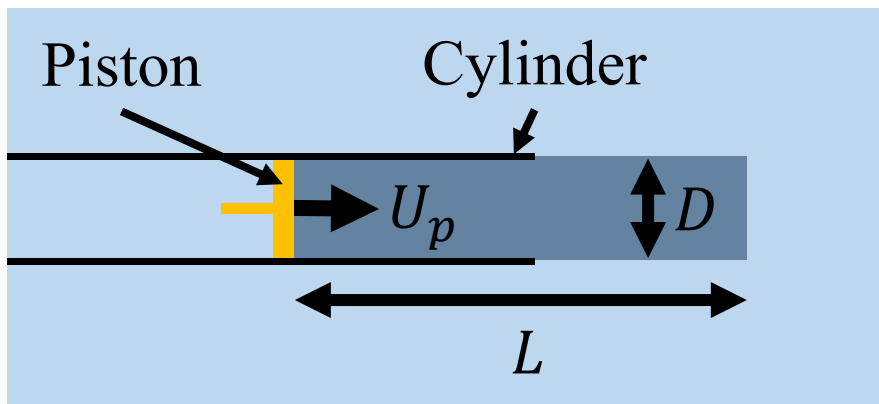
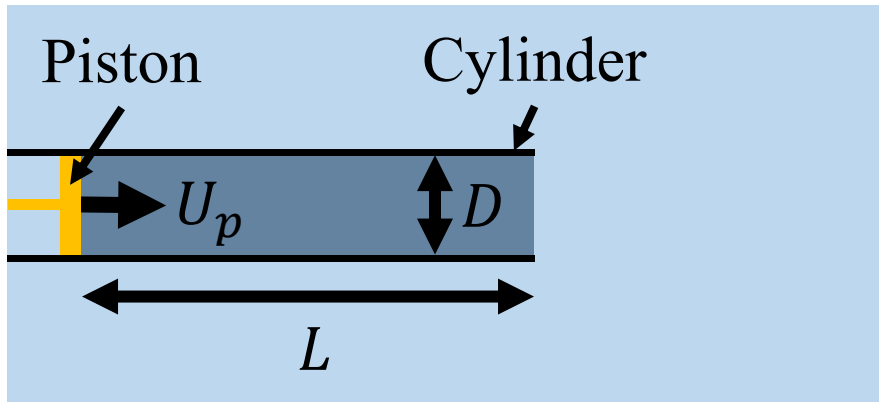
$L/D = 3.8$



$L/D = 14.5$

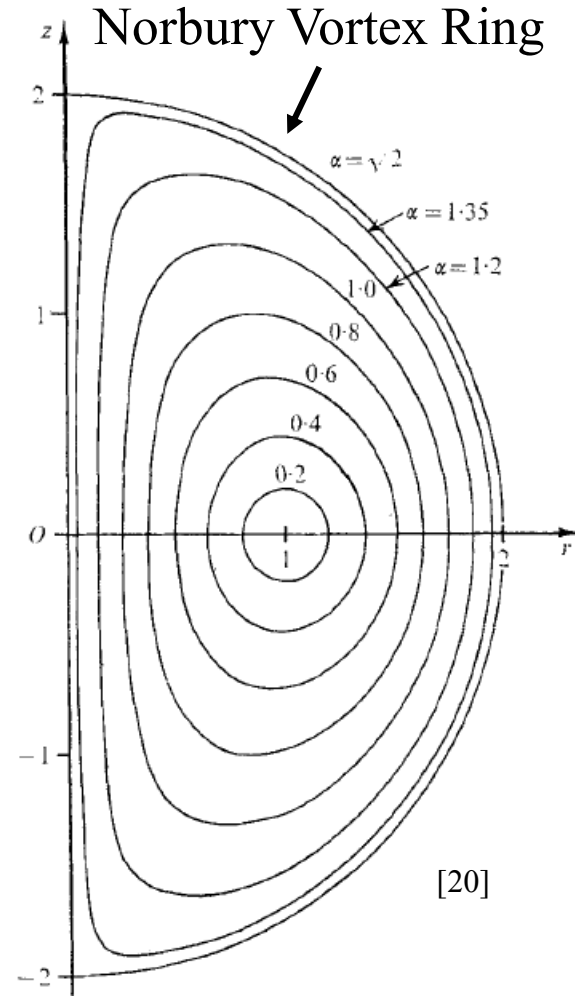
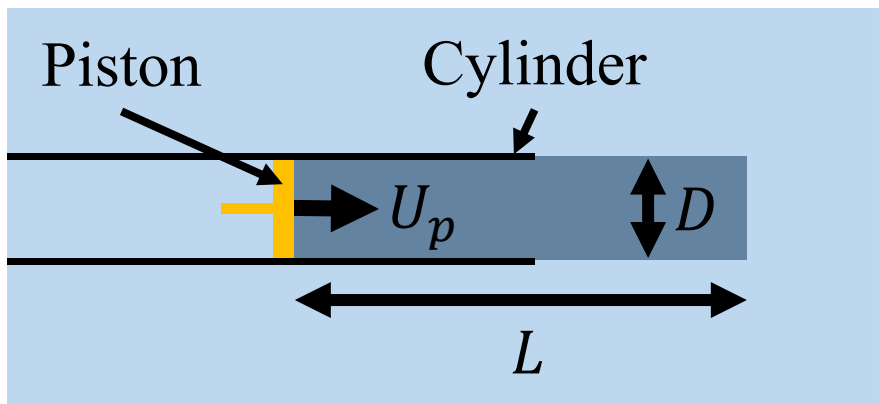
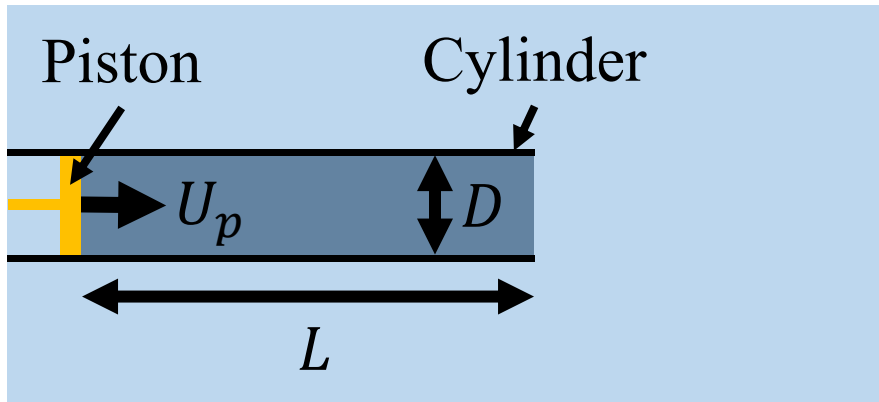


The formation number is based on analysis comparing the amount of energy supplied by the piston to the energy that can reside in the ring.



<u>Slug Flow</u>	
$E = \frac{1}{8} \pi D^2 L U_p^2$	
$\Gamma = \frac{1}{2} L U_p$	
$I = \frac{1}{4} \pi D^2 L U_p$	
$U_{tr} = \frac{\partial E}{\partial I} = \frac{1}{2} U_p$	

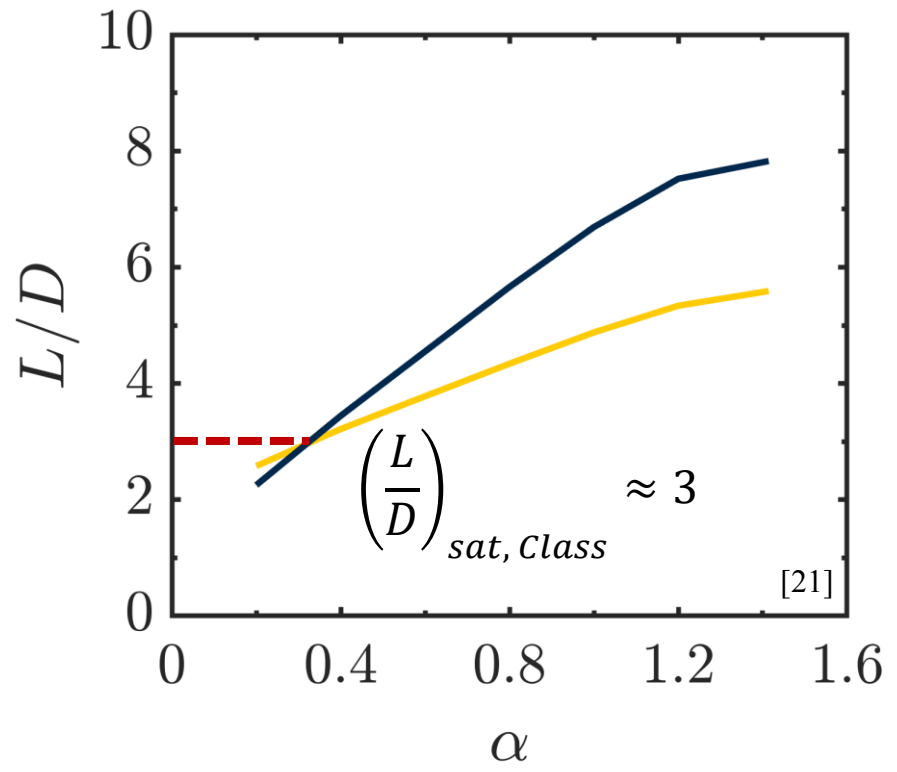
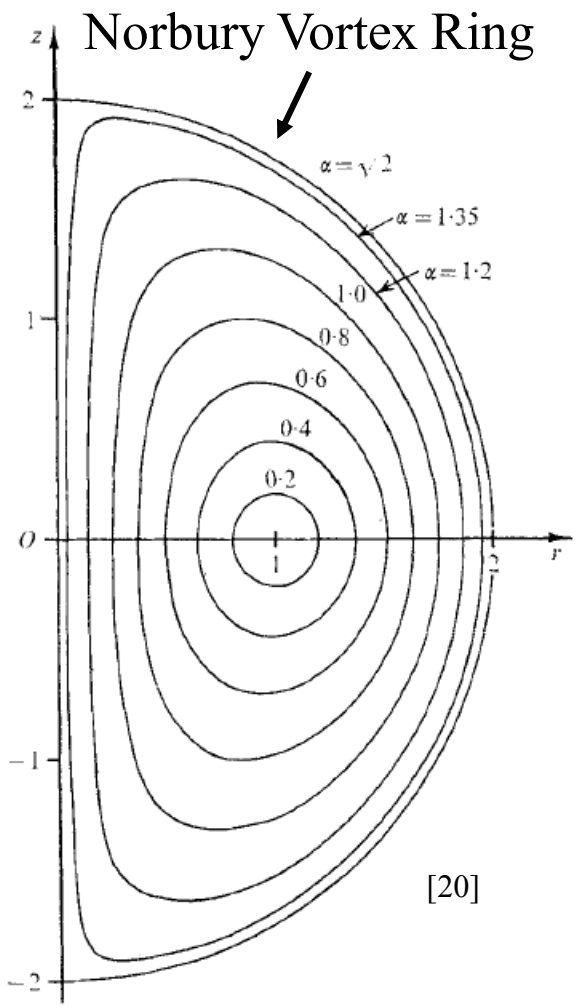
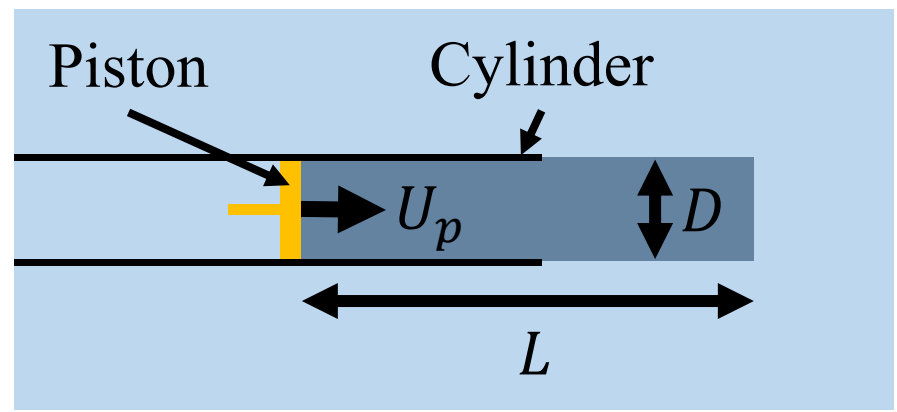
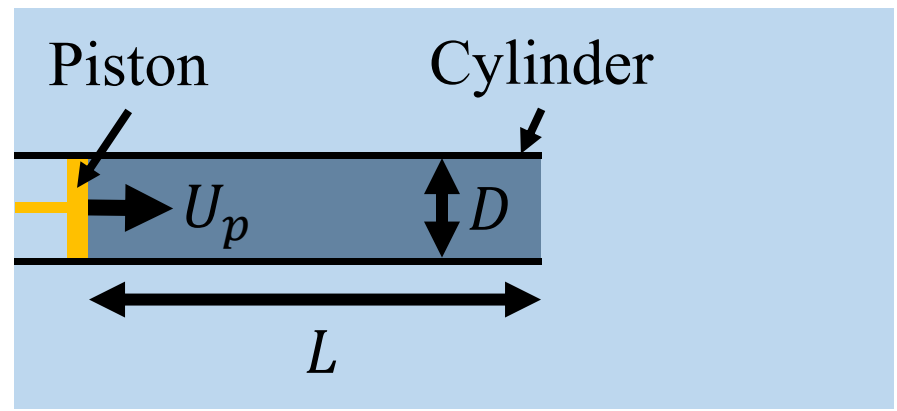
The formation number is based on analysis comparing the amount of energy supplied by the piston to the energy that can reside in the ring.



<u>Slug Flow</u>	<u>Norbury Vortex Ring</u>
$E = \frac{1}{8} \pi D^2 L U_p^2$	$E = (\Omega \alpha l)^2 l^3 E_N$
$\Gamma = \frac{1}{2} L U_p$	$\Gamma = (\Omega \alpha l) l \Gamma_N$
$I = \frac{1}{4} \pi D^2 L U_p$	$I = (\Omega \alpha l) l^3 I_N$
$U_{tr} = \frac{\partial E}{\partial I} = \frac{1}{2} U_p$	$U_{tr} = (\Omega \alpha l) U_N$ [21]

$$\frac{L}{D} = \sqrt{\frac{\pi}{2}} I_N^{\frac{1}{2}} \Gamma_N^{\frac{3}{2}} E_N^{-1} \quad \frac{L}{D} = \sqrt{\frac{\pi}{2}} I_N^{-\frac{1}{2}} \Gamma_N^{\frac{3}{2}} U_N^{-1}$$

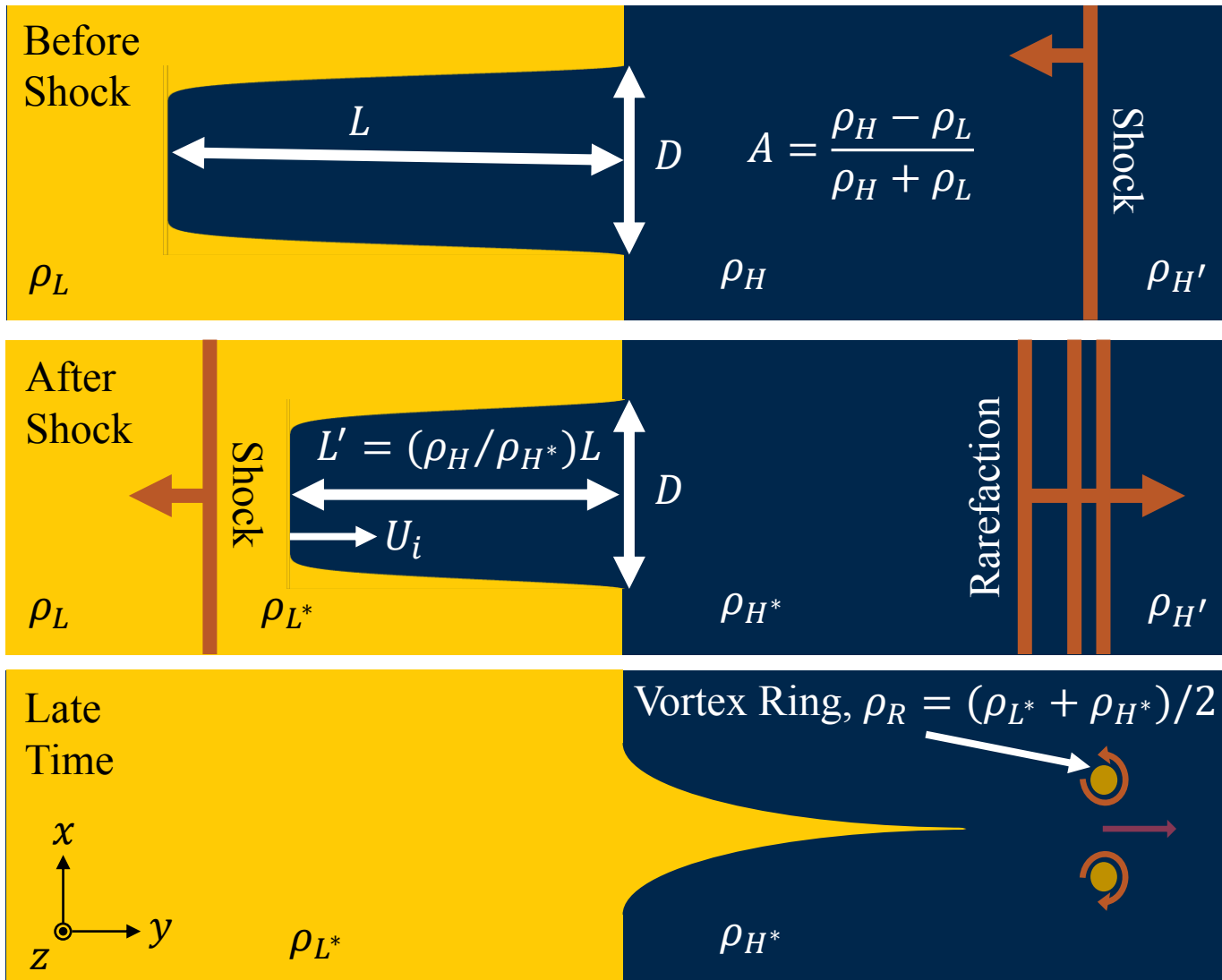
The formation number is based on analysis comparing the amount of energy supplied by the piston to the energy that can reside in the ring.



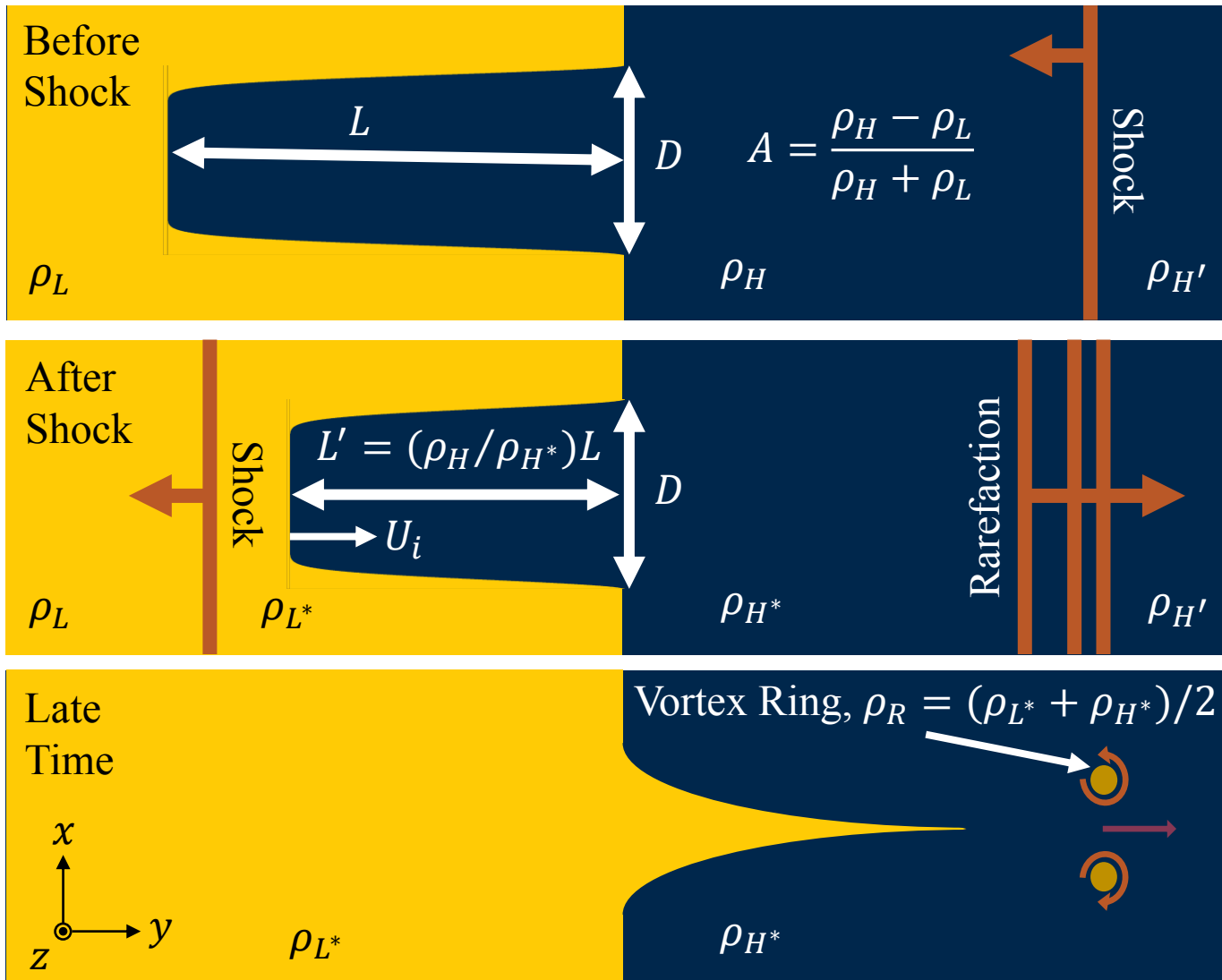
$$\frac{L}{D} = \sqrt{\frac{\pi}{2}} I_N^{\frac{1}{2}} \Gamma_N^{\frac{3}{2}} E_N^{-1} \quad \frac{L}{D} = \sqrt{\frac{\pi}{2}} I_N^{-\frac{1}{2}} \Gamma_N^{\frac{3}{2}} U_N^{-1}$$

$$3.0 \leq \left(\frac{L}{D}\right)_{sat} \leq 4.6$$

We modify the classical theory for vortex ring scaling by considering the strength of the shock and the interfacial Atwood number.



We modify the classical theory for vortex ring scaling by considering the strength of the shock and the interfacial Atwood number.



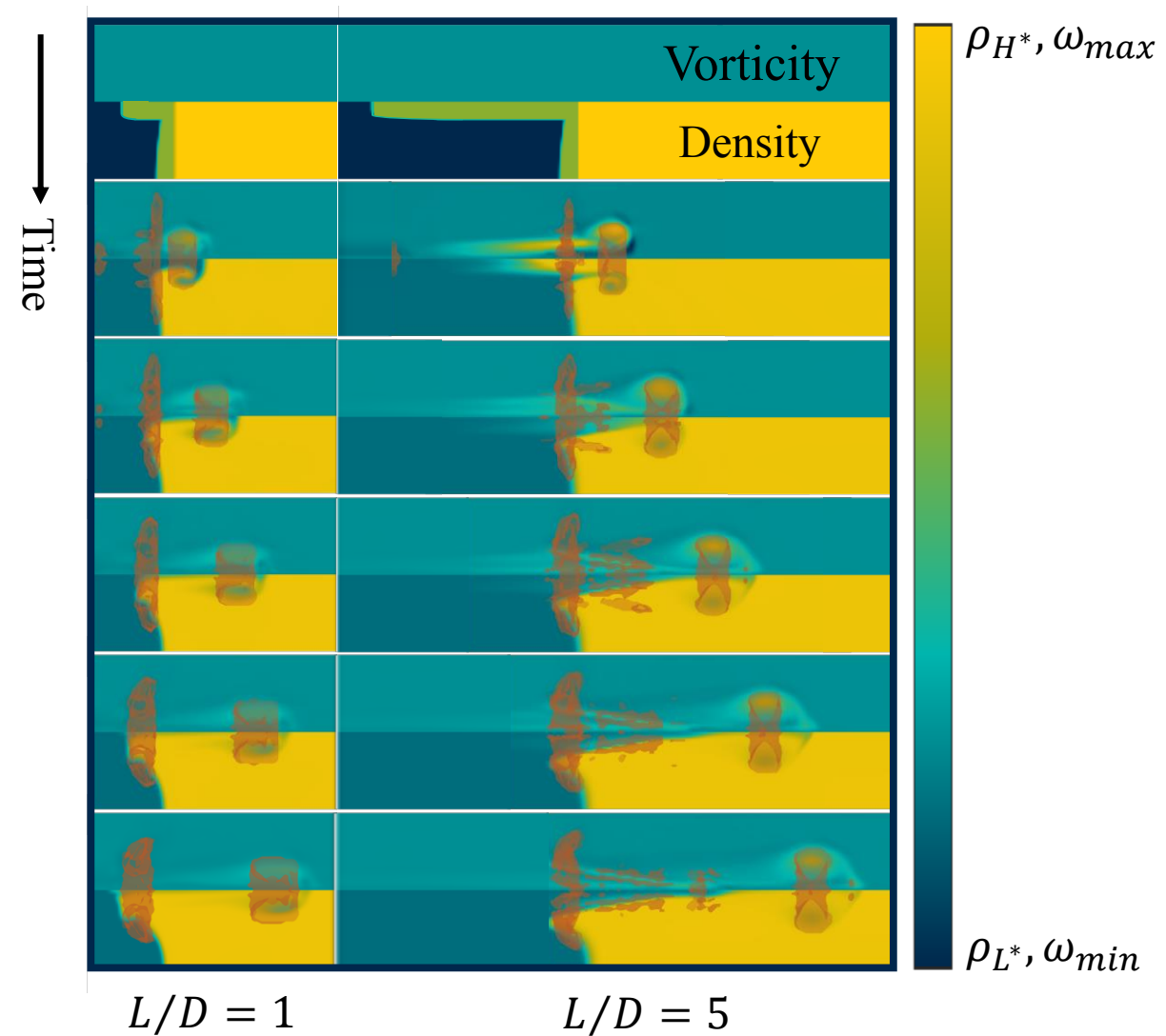
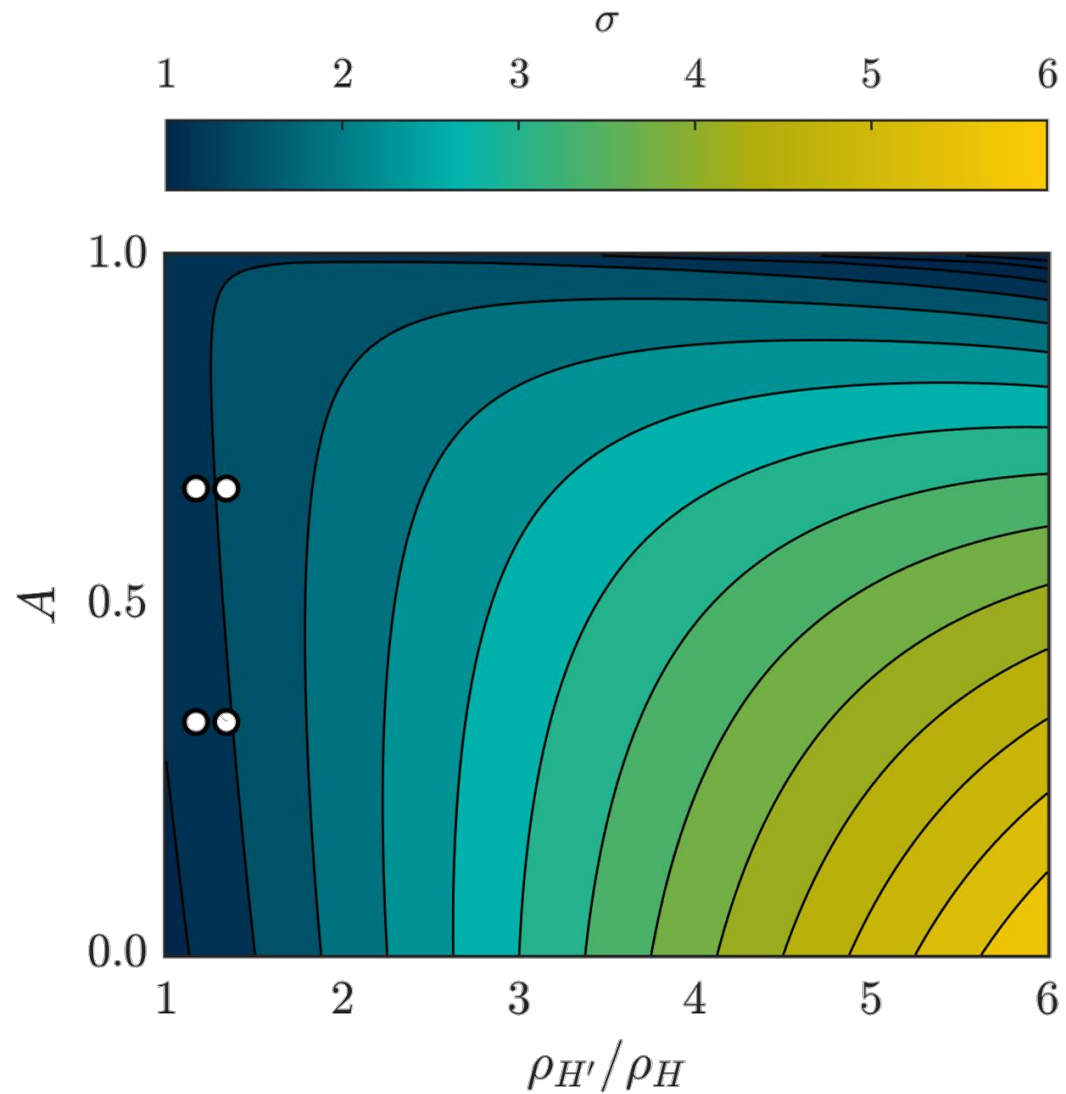
<u>Slug Flow</u>	<u>Norbury Vortex Ring</u>
$E = \rho_H \frac{1}{8} \pi D^2 L U_i^2$	$E = \frac{(\rho_{L^*} + \rho_{H^*})}{2} (\Omega \alpha l)^2 l^3 E_N$
$\Gamma = \frac{\rho_H}{\rho_{H^*}} \frac{1}{2} L U_i$	$\Gamma = (\Omega \alpha l) l \Gamma_N$
$I = \rho_H \frac{1}{4} \pi D^2 L U_i$	$I = \frac{(\rho_{L^*} + \rho_{H^*})}{2} (\Omega \alpha l) l^3 I_N$
$U_{tr} = \frac{\partial E}{\partial I} = \frac{1}{2} U_i$	$U_{tr} = (\Omega \alpha l) U_N$

$$\left(\frac{L}{D}\right)_{sat, RMI} = \sigma \left(\frac{L}{D}\right)_{sat, Class}$$

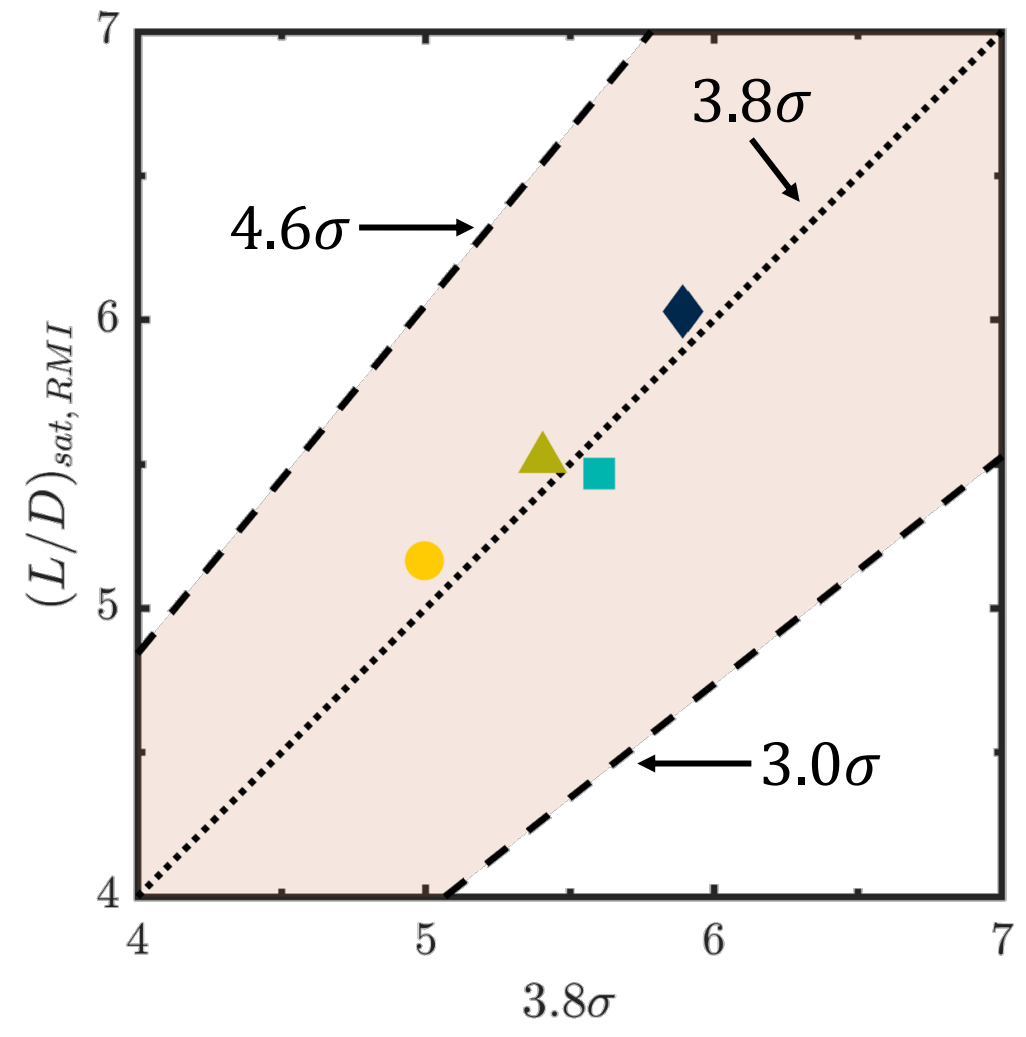
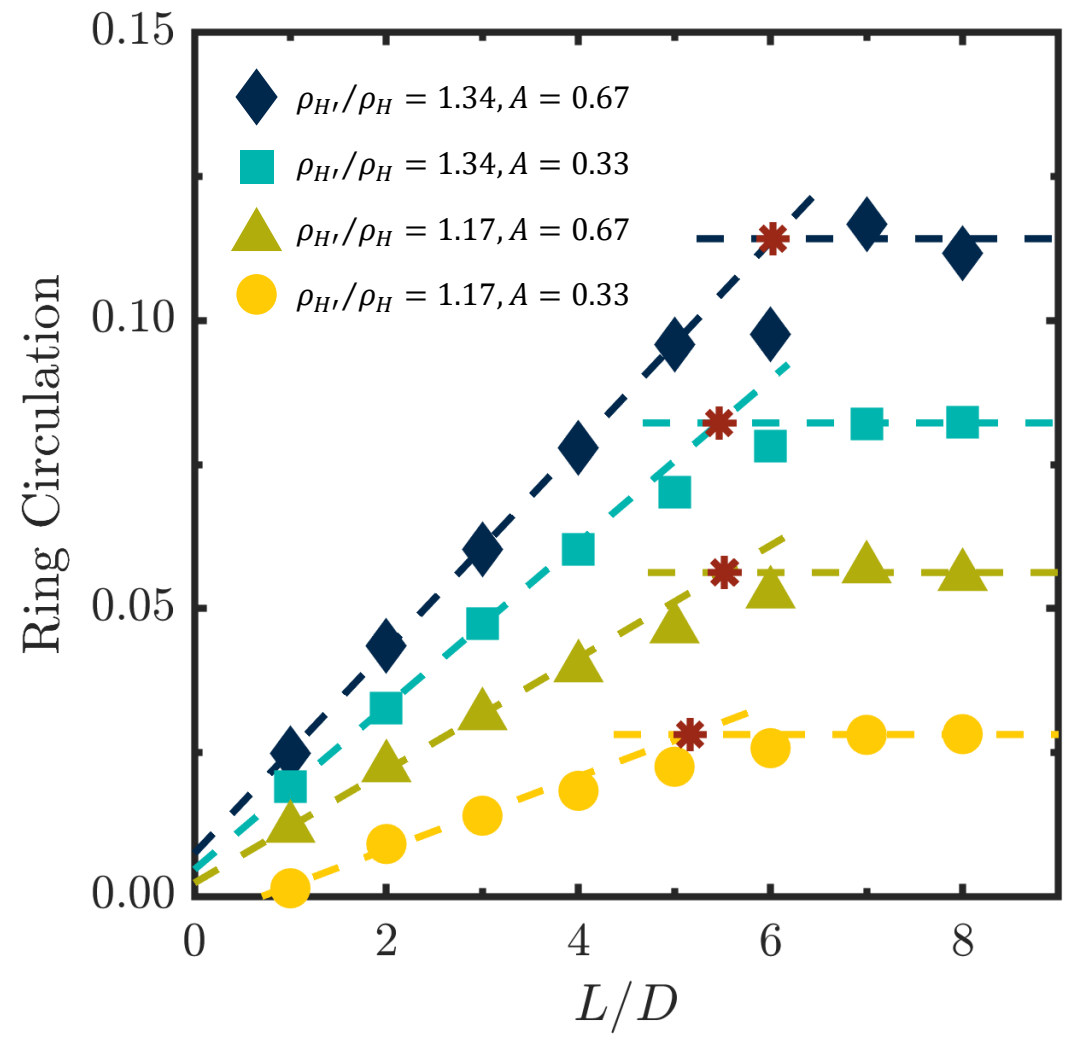
$$\sigma = \sqrt{\frac{2\rho_{H^*}}{\rho_{L^*} + \rho_{H^*}} \frac{\rho_{H^*}}{\rho_H}} = f(\rho_{H'}/\rho_H, A)$$

Multifluid Compression

The model predicts an augmented formation number, and simulations show many formation number signatures.



Simulations verify that our model captures the augmented formation number scaling of vortex rings ejected from shock-accelerated interfaces.



1. Shock waves occur in a wide range of engineering and scientific contexts including laser experiments, astrophysics, and inertial confinement fusion (ICF).
2. High-powered lasers can drive strong waves in materials, enabling their study in extreme pressure environments. We developed a method for further strengthening such shocks.
3. Shocked interfaces mix via the Richtmyer-Meshkov instability (RMI), possibly leading to the escape of high-vorticity ejecta with important implications for turbulent transitions.



1. Musci et al., Supernova hydrodynamics: a lab-scale study of the blast-driven instability using high-speed diagnostics, *The Astrophysical Journal*, 2020
2. Thornber and Zhou, Numerical simulations of the two-dimensional multimode Richtmyer-Meshkov instability, *Physics of Plasmas*, 2015
3. Kane et al., An evaluation of the Richtmyer-Meshkov instability in supernova remnant formation, *The Astrophysical Journal*, 1999
4. Chen et al., Gas dynamics of the nickel-56 decay heating in pair-instability supernovae, *The Astrophysical Journal*, 2020
5. Clark et al., Three-dimensional modeling and hydrodynamic scaling of National Ignition Facility implosions, *Physics of Plasmas*, 2019
6. Saunders et al., Experimental Observations of Laser-Driven Tin Ejecta Microjet Interactions, *Physical Review Letters*, 2021
7. Rosen et al., Laboratory-astronomy jet experiments at the omega laser facility, *Journal de Physique IV*, 2006
8. Wadas et al., A theoretical approach for transient shock strengthening in high-energy-density laser compression experiments, *Physics of Plasmas*, 2021
9. Bender et al., Simulation and flow physics of a shocked and reshocked high-energy-density mixing layer, *Journal of Fluid Mechanics*, 2020
10. Sewell et al., Time-resolved particle image velocimetry measurements of the turbulent Richtmyer--Meshkov instability, *Journal of Fluid Mechanics*, 2020
11. Soulard et al., Performance of large eddies in Richtmyer-Meshkov turbulence for weak shocks and high Atwood numbers, *Physical Review Fluids*, 2022
12. Balasubramanian et al., Experimental study of initial condition dependence on Richtmyer-Meshkov instability in the presence of reshock, *Physics of Fluids*, 2012
13. Baker et al., Fill tube dynamics in inertial confinement fusion implosions with high density carbon ablaters, *Physics of Plasmas*, 2020
14. Hammel et al., Diagnosing and controlling mix in National Ignition Facility implosion experiments, *Physics of Plasmas*, 2011
15. Haines et al., Robustness to hydrodynamic instabilities in indirectly driven layered capsule implosions, *Physics of Plasmas*, 2019
16. Blue et al., Three-dimensional hydrodynamic experiments on the national ignition facility, *Physics of Plasmas*, 2005
17. Buttler et al., Unstable Richtmyer--Meshkov growth of solid and liquid metals in vacuum, *Journal of Fluid Mechanics*, 2012
18. Thornber and Zhou, Energy transfer in the Richtmyer-Meshkov instability, *Physical Review E*, 2012
19. Gharib et al., A universal time scale for vortex ring formation, *Journal of Fluid Mechanics*, 1998
20. Norbury, A family of steady vortex rings, *Journal of Fluid Mechanics*, 1973
21. Mohseni and Gharib, A model for universal time scale of vortex ring formation, *Physics of Fluids*, 1998